Marine Geology 286 (2011) 35–50

Contents lists available at ScienceDirect

Marine Geology

journal homepage: www.elsevier.com/locate/margeo

Sea level controls sedimentation and environments in coastal caves and sinkholes

Peter J. van Hengstum [a,*], David B. Scott [a], Darren R. Gröcke [b], Matthew A. Charette [c]

[a] Centre for Environmental and Marine Geology, Department of Earth Sciences, Dalhousie University, Halifax, Nova Scotia, Canada B3H 4J1
[b] Department of Earth Sciences, Durham University, Durham, D1H 3LE, UK
[c] Department of Marine Chemistry and Geochemistry, Woods Hole Oceanographic Institution, Woods Hole, MA, 02543, USA

ARTICLE INFO

Article history:
Received 23 February 2011
Received in revised form 8 May 2011
Accepted 19 May 2011
Available online 12 June 2011

Communicated by J.T. Wells

Keywords:
cave sediments
anchialine
submarine
phreatic
vadose
sea level
Bermuda

ABSTRACT

Quaternary climate and sea-level research in coastal karst basins (caves, cenotes, sinkholes, blueholes, etc.) generally focuses on analyzing isotopes in speleothems, or associating cave elevations prior sea-level highstands. The sediments in coastal karst basins represent an overlooked source of climate and sea-level information in the coastal zone, but to accurately interpret these sediments first requires an understanding of the forcing mechanisms that emplace them. In this study, we hypothesize that coastal karst basins transition through vadose, littoral, anchialine, and finally into submarine environments during sea-level rise because groundwater and sea level oscillate in near synchrony in the coastal zone, causing each environment to deposit a unique sedimentary facies. To test this hypothesis, the stratigraphy in twelve sediment cores from a Bermudian underwater cave (Green Bay Cave) was investigated and temporally constrained with twenty radiocarbon dates. The results indicate that we recovered the first succession spanning the entire Holocene from an underwater cave (~13 ka to present). The sediments were characterized with X-radiography, fossil remains, bulk organic matter, organic geochemistry ($\delta^{13}C_{org}$, C:N), and grain size analysis. Four distinct facies represent the four depositional environments: (i) vadose facies (>7.7 ka, calcite rafts lithofacies), (ii) littoral facies (7.7 to 7.3 ka: calcite rafts and mud lithofacies), (iii) anchialine facies (7.3 to 1.6 ka: slackwater and diamict lithofacies), and (iv) submarine facies (<1.6 ka: carbonate mud and shell hash lithofacies). The onset and duration of these sedimentary depositional environments are closely linked to Holocene sea-level rise in Bermuda, indicating that sea level controls environmental development in coastal karst basins. Finally, we present a conceptual model for interpreting the sediments and environments in coastal karst basins as a result of sea-level change.

1. Introduction

In general, cave-based reconstructions of Quaternary climate and sea levels can be organized into two areas of research. Most commonly, isotopes (e.g., $\delta^{13}C$, $\delta^{18}O$) preserved in speleothems like stalagmites or flowstones provide climate proxies (Yuan et al., 2005; Wang et al., 2008; Medina-Elizalde et al., 2010), or interrupted growth patterns or worm-encrusted layers on speleothems provide a surrogate for cave flooding and sea-level highstands (e.g., Harmon et al., 1981; Richards et al., 1994; Surić et al., 2005; Dutton et al., 2009; Dorale et al., 2010). Alternatively, cave elevations are related to prior sea-level highstands because caves often develop at the mildly acidic halocline or mixing zone in the groundwater, which oscillates in near synchrony with sea level in the coastal zone (Mylroie and Carew, 1988; Mylroie and Carew, 1990; Florea et al., 2007; Mylroie, 2008). The term *coastal karst basins* refers to the myriad of basin-like features that develop from long-term dissolution processes (speleogenesis) on carbonate platforms, such as sinkholes, cenotes, blueholes, and caves, all of which have been repeatedly flooded and drained by oscillating Quaternary sea levels. Sediment records are the primary targets of sea level and climate information in other coastal environments, yet the sediments in coastal karst basins are an over looked resource of climate and sea level information. However, sedimentation in coastal karst basins remains poorly understood, and has yet to be related to a broader forcing mechanism.

The environments that exist within coastal karst basins are not arbitrary. In contrast, their environments can be systematically divided into different groups, depending first on whether the cave is in the vadose (unsaturated) or phreatic (saturated) zone. Any coastal karst basin in the vadose zone can be described as being a *vadose* environment. Continuing below the groundwater table into the phreatic zone, Stock et al. (1986) originally classified modern phreatic coastal caves as littoral, anchialine, or submarine. These definitions were subtly expanded by van Hengstum and Scott (2011) so that different cave environments could be quantitatively distinguished based on sedimentary and microfossil characteristics. It is important to consider that all aquatic coastal karst

* Corresponding author at: Woods Hole Oceanographic Institution, Woods Hole, MA, 02543, USA. Tel.: +1 508 289 3985.
E-mail address: vanhengstum@whoi.edu (P.J. van Hengstum).

0025-3227/$ – see front matter © 2011 Elsevier B.V. All rights reserved.
doi:10.1016/j.margeo.2011.05.004

basins are open-systems with subterranean connection to the ocean, unless empirically proven otherwise in individual cases. This is because porous karst allows for uninhibited circulation of groundwater through coastal karst basins, and the groundwater itself can be divided into two general watermasses: the upper meteoric lens versus the lower saline groundwater.

Littoral environments exist when the groundwater table or sea level is within the cave passage (Fornós et al., 2009; Dorale et al., 2010). *Anchialine* environments are dominated by terrestrial influences, such as the influx of terrestrial sediment or hydrogeologically by a meteoric lens (Schmitter-Soto et al., 2002; van Hengstum et al., 2010). Saline groundwater or seawater floods *submarine* environments, which cause marine processes to dominate the environment, and any physical exits that open into the ocean will obviously be flooded by sea level (e.g., Airoldi and Cinelli, 1996; Yamamoto et al., 2010). This classification scheme is independent of speleogenesis, and focuses solely on environmental conditions within coastal karst basins. All these environments can be observed with respect to the modern position of sea level on coastal karst platforms, but they have not been linked in succession.

Three critical ideas have been proposed for coastal karst basins. First, as introduced above, discrete environments exist in these basins, each with individual environmental and hydrogeological characteristics (Holthuis, 1973; Stock et al., 1986; van Hengstum and Scott, 2011). Second, these basins provide accommodation space for sediments, and their deposition is not yet related to a broader forcing mechanism or incorporated into a unifying theory (Ford and Williams, 1989; Teeter, 1995; Alverez Zarikian et al., 2005; White, 2007; Gischler et al., 2008; van Hengstum et al., 2010; Yamamoto et al., 2010). And third, sea-level change causes a concomitant change in the position of the coastal aquifer, which causes environmental change in caves and sinkholes themselves (Shinn et al., 1996; Ginés and Ginés, 2007; Mylroie, 2008; Gabriel et al., 2009; van Hengstum et al., 2009a). We argue that all these separate ideas are inextricably linked.

We hypothesize that glacioeustacy controls environmental evolution and sedimentation patterns within coastal karst basins (Fig. 1). More specifically, sea-level rise will force coastal karst basins to systematically transition from vadose environments during a low-stand scenario, into littoral, then anchialine, and finally into submarine environments during a sea-level highstand. This framework allows each environment to retain the spatially variable sedimentary and environmental patterns that are observed along modern coastlines, yet sea level becomes the external force driving sedimentary and environmental development in coastal karst basins over time. The purpose of this study is to test this hypothesis in a modern phreatic coastal cave, which has been flooded by eustatic sea-level rise during the Holocene.

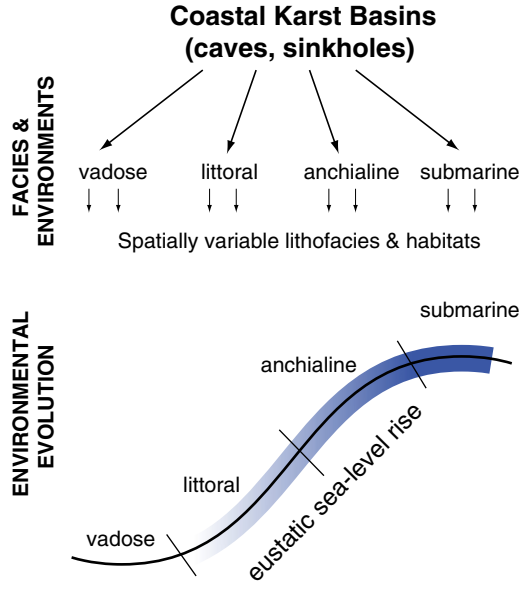

Fig. 1. Environments and facies in coastal karst basins, and their evolution during a transgressive systems tract.

2. Regional setting

Bermuda contains a basalt core overlain with karst, characterized by alternating eolianites (~90%) and paleoesols (~10%) that developed during late Quaternary sea-level highstands and low-stands, respectively (Bretz, 1960; Land et al., 1967; Vacher et al., 1989; Mylroie et al., 1995b; Vacher et al., 1995). This stratigraphy is a Carbonate-Cover Island according to the Carbonate Island Karst Model (Mylroie and Mylroie, 2007). Caves are common in Bermuda, but are most abundant on the isthmus between Castle Harbor and Harrington Sound in the diagenetically-mature Walsingham Formation (Land et al., 1967; Mylroie et al., 1995b). It is generally thought that Bermuda's caves formed through three processes: (a) phreatic dissolution in a paleo-meteoric lens during sea-level highstands, (b) vadose dissolution concentrated at the basalt–eolianite contact during sea-level lowstands, and (c) subsequent modification by collapse events (Palmer et al., 1977; Mylroie et al., 1995b). These processes have created large cave chambers connected by fissures, with sediment accumulating in structural depressions on cave floors.

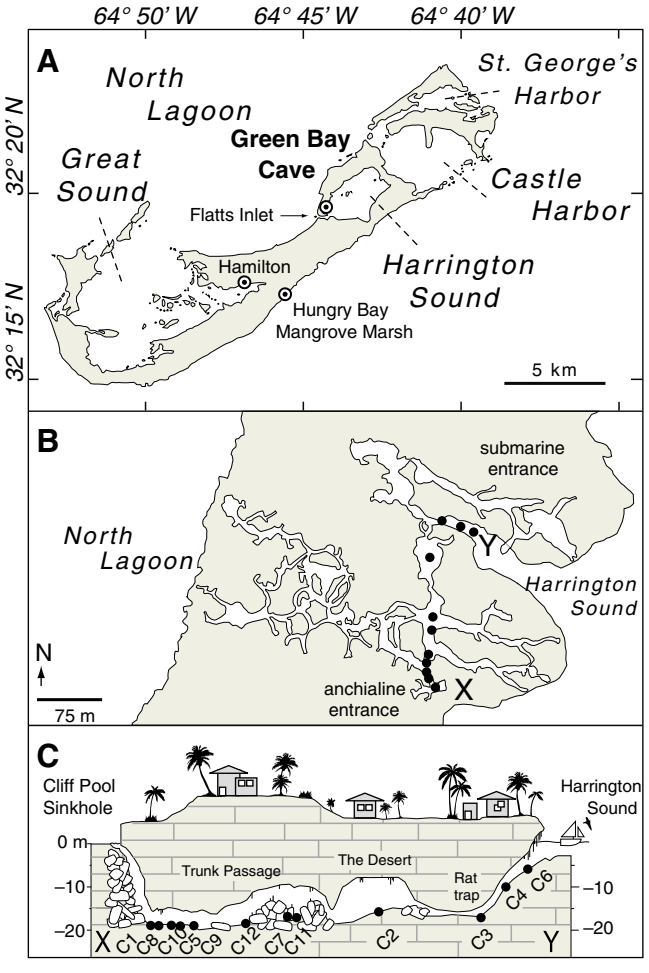

Fig. 2. A: Regional map of Bermuda with location of GBC. B: Primary cave passages and location of transect X to Y in GBC. C: Location of cores collected on SCUBA along the X to Y transect.

This study focuses on Green Bay Cave (GBC), which is located on the northeastern shore of Harrington Sound (Fig. 2). GBC has two entrances connected by almost 300 m of flooded cave: an anchialine sinkhole entrance at Cliff Pool Sinkhole, and a submarine cave entrance opening below sea level into Harrington Sound. This geomorphology provides a perfect natural laboratory to investigate the differences between anchialine and submarine environments. van Hengstum and Scott (2011) differentiated the modern environments in GBC using a multi-proxy approach (foraminifera, sedimentology, C:N, and $\delta^{13}C_{org}$), indirectly suggesting that cave environments could also be distinguished in the stratigraphic record.

Hydrogeologically, GBC is almost entirely flooded by groundwater. A thin, brackish meteoric lens in Cliff Pool Sinkhole has an elevation within ~60 cm of sea level (salinity >20 ppt, van Hengstum and Scott, 2011). This meteoric lens is buoyed on saline groundwater that is flooding the entire cave and tidally exchanged with Harrington Sound through the submarine cave entrance. Groundwater current velocities can reach 1.5 m s^{-1} during peak tidal flow at the submarine entrance (Cate, 2009), but are very low throughout the rest of the cave. Tidal amplitudes in both Harrington Sound and GBC are diminished relative to other Bermudian coastal lagoons because the exchange of seawater between the ocean and Harrington Sound is severely restricted through Flatts Inlet (Morris et al., 1977). This inlet has a sill at ~2.25 m below sea level (mbsl), which may have been shallower before excavation by colonial dredging or local currents.

Bermuda's sea-level history has attracted considerable scientific interest (Redfield, 1967; Harmon et al., 1981; Vacher and Hearty, 1989; Hearty et al., 1999), as some authors maintain that Bermuda nearly observes eustacy because the islands have remained tectonically and glacio-isotatically stable throughout the Quaternary (Olson and Hearty, 2009). This perspective has been questioned by others (Vacher and Rowe, 1997; Bowen, 2010), and numerical modeling suggests that Bermuda is considerably affected by ice-loading in North America (Milne and Mitrovica, 2008). However, geological evidence confirming glacioisostatic adjustment of the Bermuda platform remains unavailable. Evidence for the sea-level history of Bermuda over the last 12 ka is predominantly based on basal terrestrial (freshwater) peat, which is a *maximum* sea-level indicator only (Redfield, 1967; Neumann, 1971; Vollbrecht, 1996). In contrast, Holocene sea-level index points based on basal brackish water peat in Bermuda are considerably fewer (Ellison, 1993; Javaux, 1999). The oldest reliable basal brackish peat is positioned at −9.9 mbsl and radiocarbon dated to 6.9 ka (Vollbrecht, 1996), and is followed by two closely spaced points at approximately −5.5 mbsl that are radiocarbon dated to 5.6 ka (Ellison, 1993; these data were recalibrated with Intcal09). This is significant for GBC because the average depth of the cave floor is approximately −20 mbsl, and was thus flooded by Holocene sea-level rise.

3. Methods

Twelve percussion cores (5 cm diameter) were collected on SCUBA (self-contained underwater breathing apparatus) along a transect from the submarine cave entrance to the anchialine cave entrance (Fig. 2C). All cores were extruded, logged, and sampled at 5 to 10 mm intervals in field, but cores 1 to 5 were first shipped back to Bedford Institute of Oceanography (Nova Scotia, Canada) for X-radiography before sampling. Twenty radiocarbon dates were obtained on the cores (Table 1) by dating shell material from marine intervals and terrestrial organic matter during non-marine intervals (to avoid bias from a hard water effect). Furthermore, several additional basal brackish peats were collected from the Hungry Bay Mangrove Marsh with a Davis Corer (to avoid bias from autocompaction) to expand the regional database of Holocene sea-level index points (Appendix 1). All new radiocarbon dates reported here, along with dates reported from the literature, have been calibrated using IntCal09 and Marine09 (Reimer et al., 2009), applying a reservoir correction with local offsets from the global mean (ΔR of -48 ± 40 yrs) to biogenic carbonates (Druffel, 1997).

Particle size analysis was completed on a Beckman Coulter LS 230 employing the Fraunhofer optical model, which measures particles with diameters from 0.04 to 2000 μm with a precision of <2 μm. Bulk sediment samples, including both carbonates and organics, were measured to retain a complete signature of environmental processes (Donnelly and Woodruff, 2007; Donato et al., 2009). Particle size distributions (PSD) were continuously measured downcore, log transformed to the phi-scale, interpolated, and plotted as a color surface plot (Beierle et al., 2002; van Hengstum et al., 2007; van Hengstum et al., 2010). Paleontological remains (e.g., gastropods, bivalves, foraminifera, fish bones) were microscopically examined in replicate sediment samples to assess downcore biofacies.

Organic matter availability is arguably one of the most important variables influencing environmental development in coastal karst basins (Fichez, 1990; Pohlman et al., 1997; Panno et al., 2004). Therefore, understanding its source, quantity, and quality is quite helpful in cave paleoenvironmental analysis (van Hengstum et al., 2009a; van Hengstum et al., 2010). The quantity of bulk

Table 1
Radiocarbon dates.

Index no.	Lab number	Core	Core interval	Material	Conventional ^{14}C age	$\delta^{13}C$ (‰)	Calibrated age (2σ)
1	OS-74175	GBC1	10 ± 0.5	Twigs	2910 ± 35	−27.27	3080 ± 130
2	OS-74176	GBC1	21.5 ± 0.5	Twigs	4190 ± 45	−24.91	4710 ± 130
3	OS-74177	GBC1	71.5 ± 0.5	Twigs	5070 ± 70	−25.89	5820 ± 165
4	OS-79473	GBC5	14.5 ± 0.5	Bivalve — *Barbatia domingensis*	645 ± 25	2.79	350 ± 95
5	OS-78020	GBC5	27.5 ± 0.5	Bivalve — *Barbatia domingensis*	1610 ± 25	0.39	1200 ± 100
6	OS-78019	GBC5	31.25 ± 0.25	Bivalve — *Barbatia domingensis*	2040 ± 25	−0.57	1670 ± 130
7	OS-78451	GBC5	38.25 ± 0.25	Bulk organics	3590 ± 30	−27.12	3900 ± 70
8	OS-74180	GBC5	46.25 ± 0.25	Bulk organics	3800 ± 40	−27.48	4200 ± 190
9	OS-74179	GBC5	49.75 ± 0.25	Bulk organics	4930 ± 45	−25.23	5670 ± 80
10	OS-80321	GBC5	51.5 ± 1	Foraminifera and ostracodes	6800 ± 50	−0.14	7360 ± 120
11	OS-79218	GBC5	61.25 ± 0.75	Foraminifera and ostracodes	7160 ± 65	−1.59	7690 ± 150
12	OS-79474	GBC5	65.25 ± 0.25	Terrestrial gastropod — *Poecilozonites*	11100 ± 65	−8.02	12,940 ± 200
13	OS-74186	GBC6	27.5 ± 0.5	Bivalve	1140 ± 40	−0.18	760 ± 110
14	OS-81363	GBC9	11.5 ± 0.5	Bivalve — *Barbatia domingensis*	595 ± 25	2.9	280 ± 140
15	OS-81364	GBC9	37.5 ± 0.5	Bivalve — *Barbatia domingensis*	2000 ± 25	0.29	1630 ± 130
16	OS-81373	GBC9	59.5 ± 0.5	Foraminifera and ostracodes	6700 ± 35	−0.72	7280 ± 110
17	OS-81365	GBC11	37.25 ± 0.25	Bivalve — *Barbatia domingensis*	2020 ± 25	0.88	1650 ± 130
18	OD-81366	GBC11	41 ± 0.75	Foraminifera and ostracodes	7030 ± 30	0.42	7560 ± 100
19	OS-81369	GBC11	46.75 ± 0.75	Foraminifera and ostracodes	7210 ± 40	−0.93	7720 ± 120
20	OS-81367	GBC12	29.5 ± 0.5	Bivalve — *Barbatia domingensis*	1630 ± 25	−0.1	1230 ± 100

organic matter (wt. %) was measured downcore by loss on ignition at 550 °C for 4.5 h, with error on replicate samples less than ± 2% (Appendix 1). This is the typical precision for the method (Heiri et al., 2001).

Isotopic ($\delta^{13}C_{org}$) and elemental (C:N) analysis provides a proxy for the source and quality of bulk organic matter, respectively (Lamb et al., 2006). Sediment samples from cores 1, 2, 3, 5, and 9 were first subjected to a 10% HCl carbonate digestion for 24 h, rinsed to neutrality, then dried and powdered. Stable carbon isotopes are reported in conventional delta (δ) notation relative to the standard Vienna PeeDee Belemnite (VPDB) with a precision of ± 0.2‰. Some uncertainty in the $\delta^{13}C_{org}$ and C:N values may be introduced to the final values from organic matter derived from brackish aquatic plants (algae, phytoplankton) in Cliff Pool Sinkhole with a similar isotopic value to C_3 terrestrial plants (Sánchez et al., 2002; Schmitter-Soto et al., 2002; Lamb et al., 2006; van Hengstum et al., 2010). However, this is likely minor considering the small size of the sinkhole available for primary productivity, and that $\delta^{13}C_{org}$ and C:N have been used to effectively identify marine versus terrestrial organic matter in other environments (e.g., Thornton and McManus, 1994; Voβ and Struck, 1997; Kemp et al., 2010). In general, this is because organic matter in terrestrial environments dominated by C_3 plants has a more depleted carbon isotopic signature and higher C:N ratio (nitrogen-poor) than marine organic matter (Lamb et al., 2006). The modern $\delta^{13}C_{org}$ terrestrial endmember in GBC is (δX_t) is −26.7‰, and the marine endmember is (δX_m) is −16.8‰ (van Hengstum and Scott, 2011), so the relative proportion of terrestrial (F_t) versus marine (F_m) organic matter in GBC sediment was estimated using a two-source isotope mass balance (Thornton and McManus, 1994; Voβ and Struck, 1997; Ogrinc et al., 2005):

$$\delta X = F_m{}^{*}\delta X_m + F_t{}^{*}\delta X_t \quad (1)$$

$$1 = F_t + F_m \quad (2)$$

4. Lithofacies

A total of 5.82 m of core was recovered, originally representing 14.4 m of sediment with a mean compaction of 58.5% (Table 2). High rates of compaction were expected because carbonate mud is the dominant sediment and may have up to 80% porosity (Enos and Sawatsky, 2003). However, rodding effects may have occurred to cores not hitting basement because of the narrow pipe diameter used (e.g., cores 3 and 4). All cave radiocarbon dates are stratigraphically ordered and sequentially date correlative lithofacies in the succession. The oldest radiocarbon date of 12.9 ka is from a *Poecilozonites* shell (terrestrial gastropod) at the base of core 5. Uncertainty on the youngest dates correspond with colonization of Bermuda in 1609 AD (Table 1).

Six lithofacies were identified based on organic matter quantity (wt. %), organic matter source ($\delta^{13}C_{org}$, C:N), PSDs, X-radiographs,

Table 2
Water depth, core recovery, and compaction of GBC cores.

Core	Water depth (m)	Recovery (m)	True thickness (m)	Compaction (%)
C1	18.9	0.74	1.94	61.9
C2	15.8	0.44	1.08	59.3
C3	16.5	0.5	1.7	70.6
C4	12.2	0.23	1.01	77.2
C5	19.5	0.68	1.33	48.9
C6	10.7	0.42	0.92	54.3
C7	19.6	0.41	0.85	51.8
C8	20.1	0.42	1.29	67.4
C9	19.8	0.65[a]	1.25	48
C10	19.8	0.5	1.34	62.7
C11	19.6	0.49	1.09	55
C12	19.3	0.34	0.62	45.2

Uncertainty of ± 0.3 m on depth measurements from gauges.
[a] Basal ~4 cm was observed before falling back into hole.

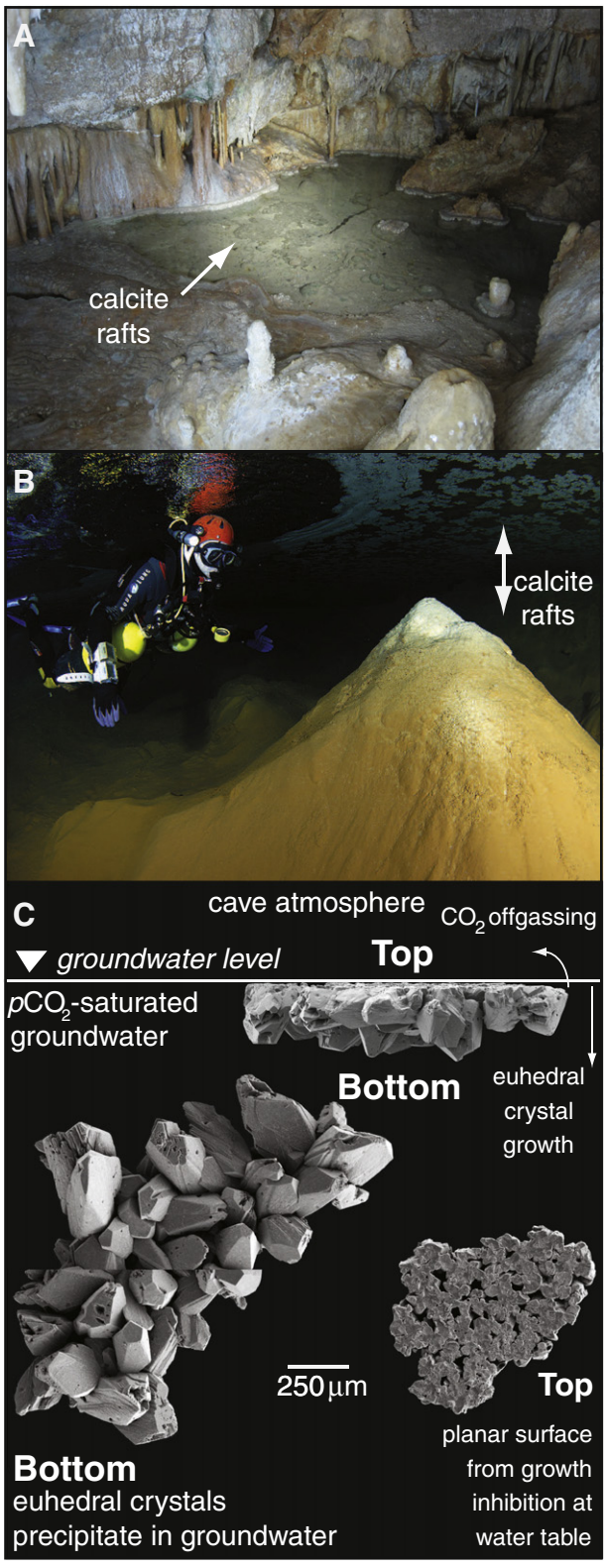

Fig. 3. A: Calcite rafts forming on a transient meteoric pool (2 m width) in a modern vadose cave environment. B: Calcite rafts forming in a littoral cave environment in Mallorca, used with permission from the National Speleological Society (adapted after Fornós et al., 2009). C: Scanning electron micrographs of calcite rafts in the littoral facies in GBC.

Table 3
Arithmetic averages for measured sedimentary characteristics in the six different lithofacies. Note that $\delta^{13}C_{org}$ and C:N were only determined on cores 1, 2, 3, 5 and 9, with percent terrestrial and marine organic matter (OM) calculated based on average $\delta^{13}C_{org}$ for the lithofacies presented in this table. Microfossils: serpulid worm tubes (sw), saline foraminifera (sf), brackish foraminifera (bf), sponge spicules (sp), brachiopods (br), and ostracodes (o).

	Organic matter (wt.%)	Granulometry				Organic geochemistry				Biofacies contents	Evidence for cave environment
		Mean (μm)	Median (μm)	Mode (μm)	Standard deviation (μm)	C:N ± 1σ	$\delta^{13}C_{org}$ ± 1σ	Percent terrestrial OM (F_t)	Percent marine OM (F_m)		
Lithofacies											
Calcite raft	2.9 ± 0.9	433.5	254.4	420	436.8	14.2 ± 1.7	−22.2 ± 3.3	54.2	45.2	*Poecilozonites* land gastropod	Vadose
Calcite raft and mud	8.4 ± 2.4	5.4	4.7	9.2	3.8	15.1 ± 3.2	−21.8 ± 2.8	48.2	51.8	sf, sw, o, sp, br	Littoral
Slackwater	21.7 ± 3.6	18.6	12.7	23.3	19.2	17.8 ± 4	−25.9 ± 2.3	91.6	8.4	bf, rare o, *Except:* core 1, 0–4 cm and core 8, 0–8 cm: sf, o	Anchialine
Diamict	22.0 ± 9.0	197.8	80.4	394.4	255.1	29.6 ± 9.6	−27.3 ± 0.8	100	0	bf, rare o	Anchialine
Shell hash	5.6 ± 1.7	270.1	98.1	626.8	357.5	10.5 ± 1.9	−19.7 ± 1.3	28.9	71.1	sf, sw, o, sp	Submarine
Carbonate mud	9.7 ± 3.1	9.4	7.7	16.6	7.2	12.1 ± 1.5	−21.1 ± 1.1	43.7	56.3	sf, sw, o, sp, br, *Barbatia domingensis*, coral	Submarine

and microfossils. In general, a basal calcite raft lithofacies devoid of microfossils initiates the cave succession, and passes up into a calcite raft and mud lithofacies containing abundant marine fossils. This is followed by diamict and slackwater deposits that are microfossil-poor, which are finally succeeded by carbonate mud and shell hash, as described in detail below.

4.1. Calcite rafts

This lithofacies constitutes a single sedimentary unit in several cores and is dominated by calcite rafts. Calcite rafts are a common autochthon in caves and morphologically distinct: one side of the raft is completely flat, whereas developed calcite rhombohedra project from the other side (Fig. 3). An air–water interface is a prerequisite for calcite rafts to precipitate. In caves, groundwater is often $CaCO_3$-supersaturated, and cave atmospheres are typically pCO_2-depressed, causing groundwater to off-gas and calcite to precipitate at the water surface (Taylor et al., 2004; Taylor and Chafetz, 2004; Fornós et al., 2009). Therefore, the side of the raft in contact with the atmosphere is flat (planar), whereas, calcite crystals grow downward into the groundwater on the opposite side of the raft (Fig. 3). Eventually, floating calcite rafts sink and become part of the sediment record when gravitational forces on the calcite raft exceed surface tension. Calcite rafts can form in both transient meteoric pools in vadose environments (Taylor and Chafetz, 2004) and at the water table in littoral cave environments (Fornós et al., 2009). The calcite raft lithofacies in GBC is the coarsest unit in the recovered strata (mean 433.5 μm), and contains the lowest bulk organic matter content (mean 2.9%). The sedimentary organic matter at the base of core 5 is predominantly terrestrial based on the strongly depleted $\delta^{13}C_{org}$ values (Table 3). $\delta^{13}C_{org}$ values become increasingly enriched in the upper part of the unit, suggesting that some marine organic matter is present. Only terrestrial invertebrates were observed in the sediment, including the Bermudian endemic gastropod *Poecilozonites* (Hearty and Olson, 2010).

The entire lithofacies has a distinctive orange hue, similar to sediments observed in Aktun Ha Cave, Mexico (van Hengstum et al., 2009a). Preliminary evidence suggests that the coloring is derived from oxidative precipitation of iron-oxide from anoxic groundwater either at the time of cave flooding, or sometime in the Holocene (van Hengstum and Charette, unpublished data).

4.2. Calcite rafts and mud

This lithofacies is thickest in core 5 (12.5 cm), but is also present in cores 9, 12, 7, and 11. A fine carbonate mud matrix (mean grain size 5.4 μm, micrite) containing calcite rafts is unique to this lithofacies. The sediment contains a mean 8.4% bulk organic matter (Table 3), which is derived from both terrestrial and marine sources based on the oscillating $\delta^{13}C_{org}$ values in core 5 between approximately −25‰ and −19‰ (Lamb et al., 2006). The calcite rafts and mud lithofacies that accumulated directly above basement eolianite (cores 12, 7 and 11) also exhibited basal orange-hued staining, which is likely related to the same geochemical mechanism affecting the calcite raft lithofacies.

Abundant marine microfossils in the unit include brachiopods, bryozoans, and cave foraminifera (e.g., *Spirophthalmidium emaciatum, Sigmoilina tenuis*). The ostracode *Paranesidea sterreri* was observed in all cores and the gastropod *Caecum caverna* was observed in core 12 (Table 3), both of which are Bermudian cave endemics (Maddocks and Iliffe, 1986; Moolenbeek et al., 1988). Two small fish bones were recovered from core 11 at 47.25 ± 0.25 cm (Fig. 4). These microfossils indicate that a permanent marine aquatic ecosystem existed in the cave during formation of this lithofacies, but the calcite rafts also indicate the presence of a water table.

4.3. Diamict

Diamicts are chaotic, poorly-sorted sedimentary units, and they exist in GBC proximal to Cliff Pool Sinkhole. The lithofacies is poorly-sorted, characterized by fine- to medium-grained sandy layers (mean 197.8 μm, mean standard deviation 255.1 μm) that alternate into layers that are framework-supported cobbles and wood fragments (e.g., core 1: 21 to 28 cm, Fig. 5). The sediments contain a mean of 22% bulk organic matter, which is 100% terrestrial based on $\delta^{13}C_{org}$ mass balance (Table 3). *Poecilozonites* shells are common in core 8 below 30 cm and at the base of core 10, intervals that are characterized by very poorly-sorted sediments with broad particle size distributions (Fig. 6). Aquatic microfossils are dominated by the brackish benthic foraminifera *Physalidia simplex* and *Conicospirillina exleyi* (Fig. 3). These taxa are known from brackish caves and sinkholes in Mexico and brackish ponds in Spain, both of which are flooded by a brackish meteoric lens (Guillem, 2007).

4.4. Slackwater

The slackwater lithofacies is a well-sorted, organic-rich unit (mean 21.7% organic matter) characterized by silt- to clay-sized particles (mean particle size 18.6 μm) with a unimodal particle size distribution (Fig. 6). Organic matter in the slackwater lithofacies is derived from terrestrial sources based on the depleted $\delta^{13}C_{org}$ values, which equates to approximately 91.6% terrestrial sources. By corollary, more marine organic matter is present in the slackwater lithofacies than the diamict lithofacies, with a mean C:N ratio of 17.8. Fine laminae can be observed

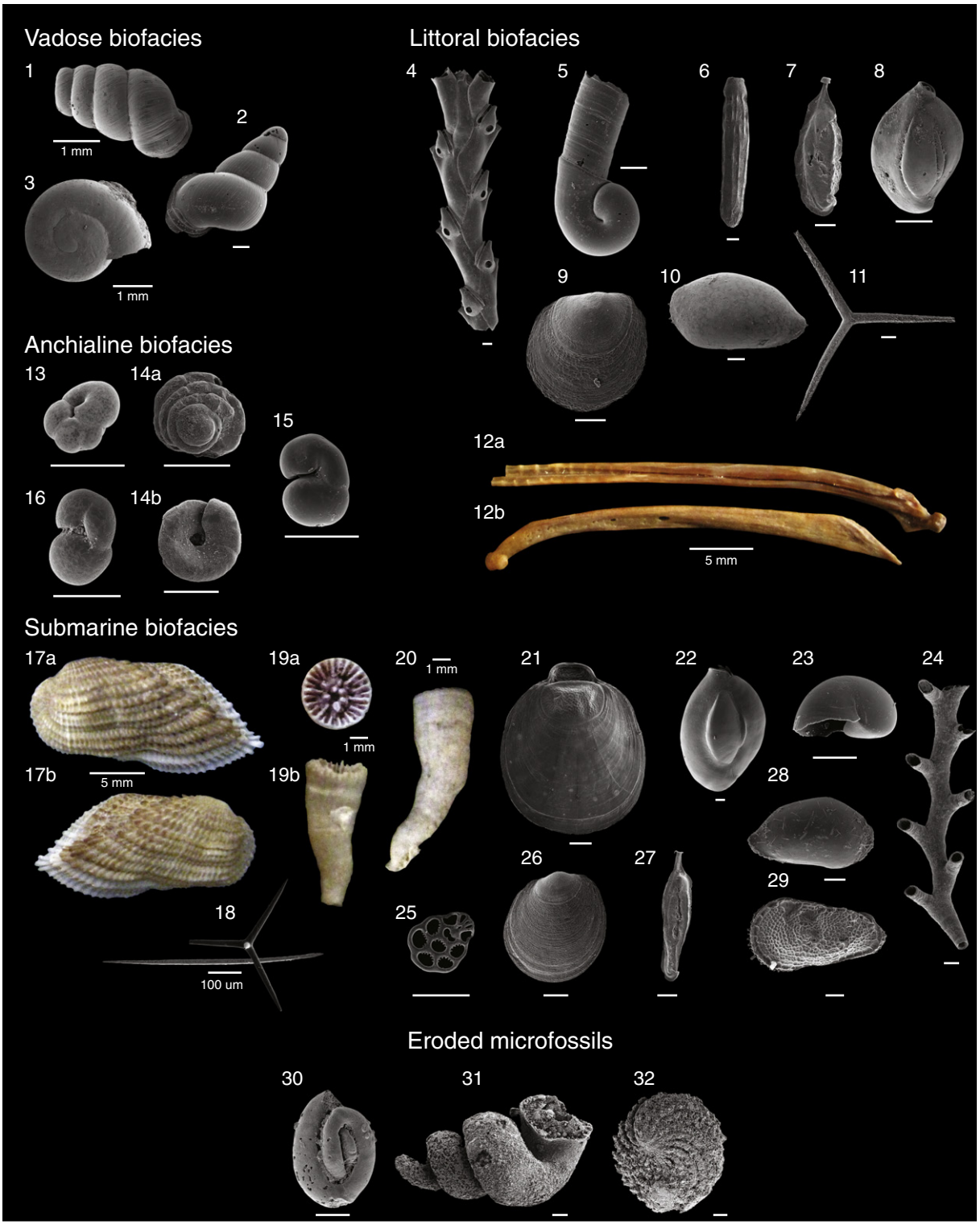

Fig. 4. Representative fossils recovered from GBC strata. **Vadose biofacies (1 to 3)**: **1, 2**, terrestrial gastropods; juvenile *Poecilozonites*, **3**; **Littoral biofacies (4 to 12)**: **4**, bryozoan; **5**, *Caecum caverna* protoconch with part of second growth stage; **6**, *Siphogenerina raphanus* (f) **7**, *Spirophthalmidium emaciatum* (f); **8**, *Quinqueloculina candeiana* (f); **9**, microbivalve; **10**, *Paranesidea sterreri* (o); **11**, sponge spicule; **12**, bones from a soft fin ray fish (a: hemitrich, b: possibly a spinous ray); **Anchialine biofacies (13 to 17)**: **13**, *Metarotaliella simplex*; **14**, *Conicospirillina exleyi* (a: dorsal, b: ventral); **15, 16**, *Physalidia simplex*; **Submarine biofaceis: 17**, bivalve *Barbatia domingenesis*; **18**, sponge spicules; **19, 20**, *Coenocyathus goreaui*; **21**, brachiopod; **22**, *Quinqueloculina candeiana*; **23**, microgastropod; **24**, bryozoan, **25**, holothurian (sea cucumber) skin ossicle; **26**, microbivalve; **27**, *Spirophthalmidium emaciatum*; **28**, *Aponesidea iliffei* (o); **29**, *Loxoconcha* sp. (o); **Eroded microfossils (30 to 32)**: **30**, *Quinqueloculina*; **31**, gastropod; **32**, *Archaias* (f). Notes: f — foraminifera, o — ostracode; scale bars represent 100 μm unless otherwise stated.

in the X-radiograph of C5 from 46 to 50 cm (Fig. 5), indicating that negligible bioturbation occurred during or after the deposition of this lithofacies.

The few microfossils present are again dominated by the brackish foraminifers *Physalidia simplex*, *Conicospirillina exleyi*, and rare ostracodes. The tops of cores 1 and 8, however, have abundant saline

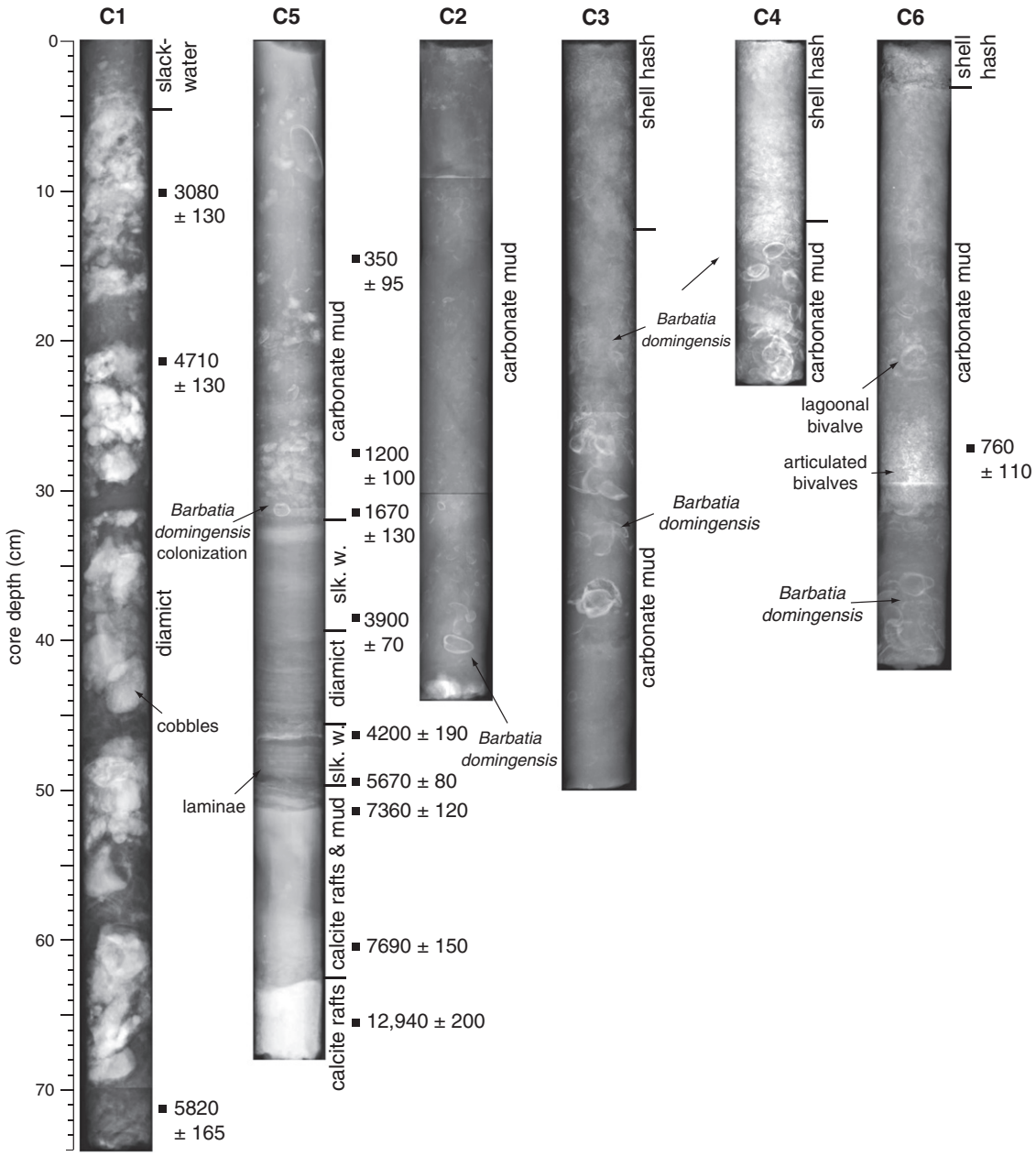

Fig. 5. X-radiographs of selected cores with lithofacies and important sedimentological characteristics noted (slk. w.: slackwater).

foraminifera consistent with the modern anchialine cave assemblage in the surface sediment of GBC (Table 3; van Hengstum and Scott, 2011). This indicates that the slackwater lithofacies present at the top of cores 1 and 8 accumulated under different hydrogeologic conditions than the slackwater lithofacies in the other cores.

4.5. Carbonate mud

A condensed unit of serpulid worm tubes and the bivalve *Barbatia domingensis* demarcates the base of the carbonate mud lithofacies; both of which are present throughout the lithofacies in all cores (Figs. 6, 7). A well-sorted carbonate mud (mean 9.4 μm) with a mean of 9.7% organic matter characterizes the unit, which is easily correlated through the cave system with a strong unimodal PSD in the coarse clay to fine silt sized-fraction (Fig. 6), and resembles most surface sediments in GBC (van Hengstum and Scott, 2011). $\delta^{13}C_{org}$ values and the C:N ratio indicate predominantly marine organic matter in the carbonate mud lithofacies (56.3%). Abundant marine microfossils are present throughout the unit, including sponge spicules, diverse benthic foraminifera, bryozoans, holothurian ossicles (sea cucumber), and brachiopods. Corallites of the Bermudian cave coral *Coenocyanthus goreaui* are present only in this lithofacies, which have been previously described from GBC (Cairns, 2000).

Two types of sedimentary layers occur within the carbonate mud lithofacies at the submarine cave entrance. First, three coarse-grained (sand) units are present in core 3 at a depth of 12 to 20 cm, each of which is 1 cm thick. Secondly, a layer of monospecific, imbricated and articulated lagoonal bivalves was found in core 6 at ~35 cm deep, which is inconsistent with the strata recovered from GBC. The PSDs indicate that carbonate mud remains the sedimentary matrix for these layers, suggesting that the background depositional setting was briefly interrupted by an external event (e.g., hurricane, tsunami).

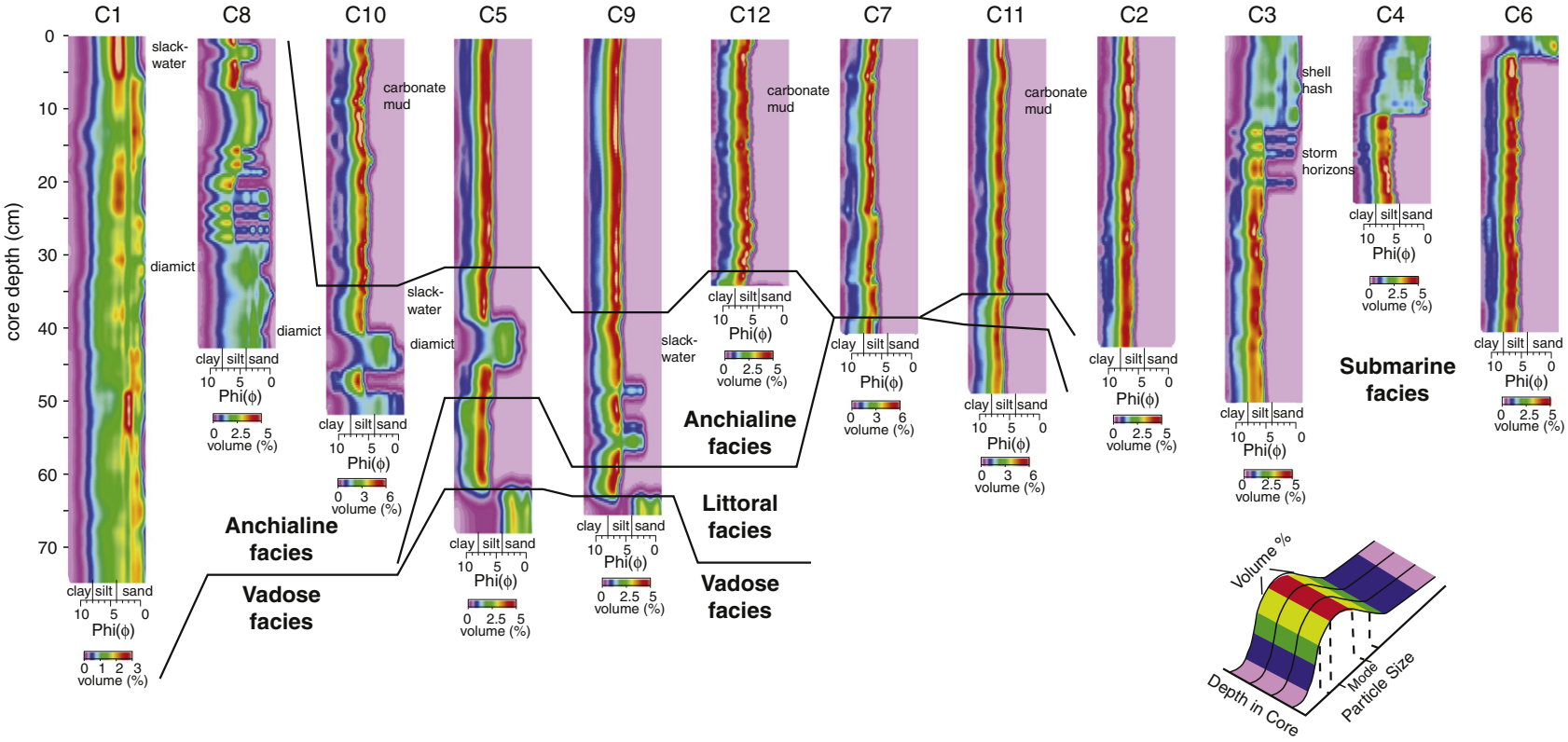

Fig. 6. Color-contoured, interpolated, particle size distributions (PSDs) from 0.4 to 2000 mm (1.3 to 10.9 ϕ), based on every downcore sediment sample (5 mm to 10 mm sampling interval).

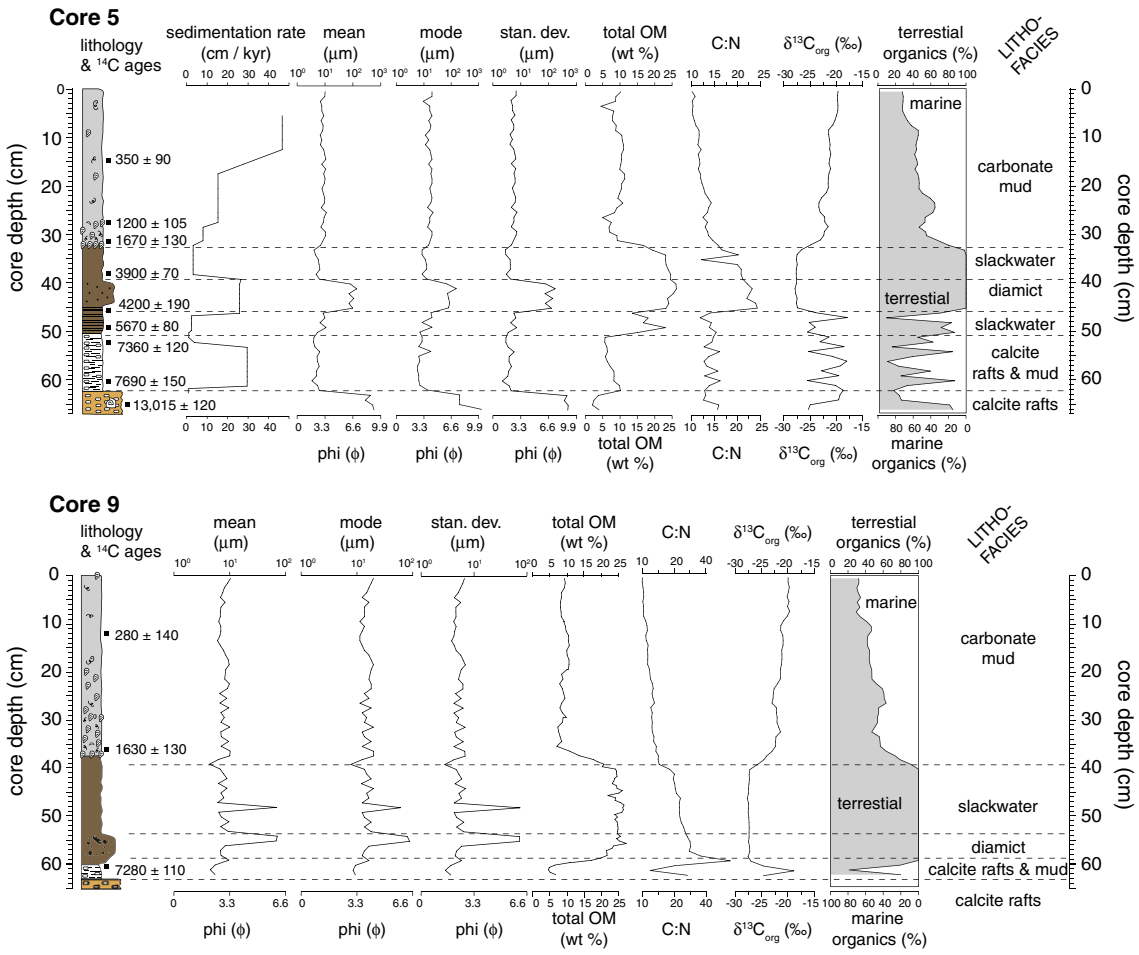

Fig. 7. Detailed sedimentological and geochemical variables from the complete Holocene cores 5 and 9. Sedimentation rates were estimated only on core 5 because it had the best age control, which were calculated by linear interpolation between radiocarbon ages. See Fig. 8 for symbol legend.

4.6. Shell hash

This lithofacies occurs in cores 3, 4 and 5 proximal to the submarine cave entrance opening into Harrington Sound. The thickest occurrence (13 cm) is present at the top of core 3. Fractured and angular fragments of lagoonal bivalve shells and debris (e.g., coral fragments) are common in the unit, which is clast-supported with a carbonate sand matrix. Additional shell material includes lagoonal foraminifera, ostracodes, bryozoans, and general shell debris, all of which have been transported into the submarine cave entrance from the lagoon in Harrington Sound. Mean $\delta^{13}C_{org}$ values (−19.7‰) and C:N ratio (10.5) indicate that the bulk organic matter

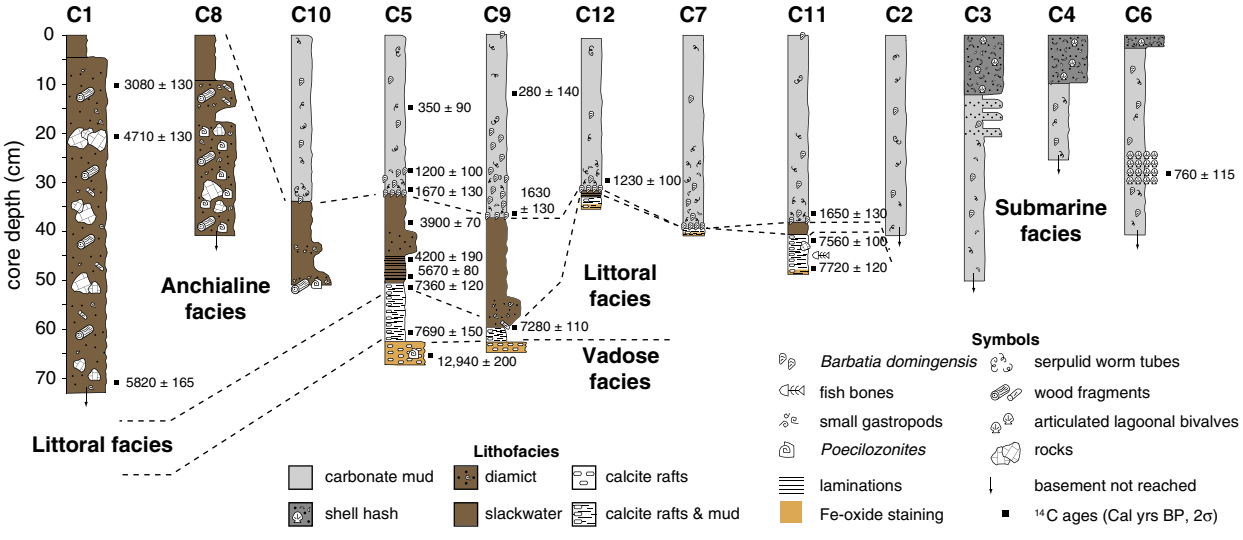

Fig. 8. Correlation and facies analysis for GBC strata.

is predominantly marine (71.4%). The shell hash lithofacies at the tops of cores 3, 4 and 5 and corresponds with the surface sediment in GBC from Harrington Sound down to the Rat Trap (van Hengstum and Scott, 2011).

5. Correlations and age

The timing of stratigraphic changes is identical between core sites, within 2σ uncertainty of the radiocarbon dates, indicating that the onset of deposition and duration of the six lithofacies are consistent throughout the cave basin (Fig. 8). These six lithofacies can be interpreted in terms of four distinct facies that represent four specific sedimentary depositional environments: (i) vadose facies (>7.7 ka, calcite rafts lithofacies), (ii) littoral facies (7.7 to 7.3 ka: calcite rafts and muds lithofacies), (iii) anchialine facies (7.3 to 1.6 ka: slackwater and diamict lithofacies), and (iv) submarine facies (<1.6 ka: carbonate mud and shell hash lithofacies). Only one radiocarbon date was available for the vadose facies because of the very minimal shell or organic matter preserved in the calcite raft lithofacies. However, a *Poecilozonites* shell provides a basal date of 12.9 ka for the succession at (Fig. 8). The contact between the vadose and littoral facies was dated twice (cores 5 and 11) and the dates provided a similar age for the transition at ~7.7 ka. The contact between the littoral and anchialine facies was dated in cores 5, 9, and 11, but the youngest age for the contact is from cores 5 and 9 at ~7.3 ka. We infer that the littoral facies rapidly accumulated in ~400 yrs, persisting slightly longer at the sites of cores 5 and 9 than at core 11. Inside the cave at the sites of cores 5 and 9, deposition of the anchialine facies began at 7.3 ka ago and continued for ~5.7 ka, but the anchialine facies persists until presently near Cliff Pool Sinkhole based on the surface sample investigation (van Hengstum and Scott, 2011). The contact between the anchialine and submarine facies was dated in three cores (5, 9, and 11), all of which produced a similar result of ~1.6 ka.

Linear interpolation between the radiocarbon dates indicates variable sedimentation rates in the successions. In the anchialine facies for example, 8 cm of sediment (38 to 46 cm) in core 5 accumulated in 0.3 ka, whereas, 4 cm of sediment (46 to 50 cm) accumulated in 1.5 ka (Fig. 7). Shifting sedimentation patterns were also observed in the submarine facies. Bivalves from slightly above (1 to 2 cm) the 1.6 ka contact in core 12 and core 5 replicated a slightly younger result of 1.2 ka, suggesting lower sedimentation rates in the cave basin at the onset of the submarine facies. However, the sedimentation rates for the carbonate mud lithofacies in GBC (from ~15 to 40 cm ka^{-1}) are comparable to the sedimentation rates for a carbonate mud lithofacies in a Japanese submarine cave (21.1 to 42 cm ka^{-1}, Omori et al., 2010). The basal contact of the shell hash lithofacies is not constrained, but the unit accumulated after 0.76 ka, based on a dated bivalve in core 6.

6. Discussion: environmental development in Green Bay Cave

Ford and Williams (1989) considered that cave entrance deposits separate from cave interior deposits, and categorized cave sedimentary constituents as allogenic or autogenic. This classification system is limited for comparing vadose and phreatic sediments within an environmental context through geologic time and geographical space, but nevertheless it remains the primary classification system for cave sediments through lack of a suitable alternative. In our view, four main environments (vadose,

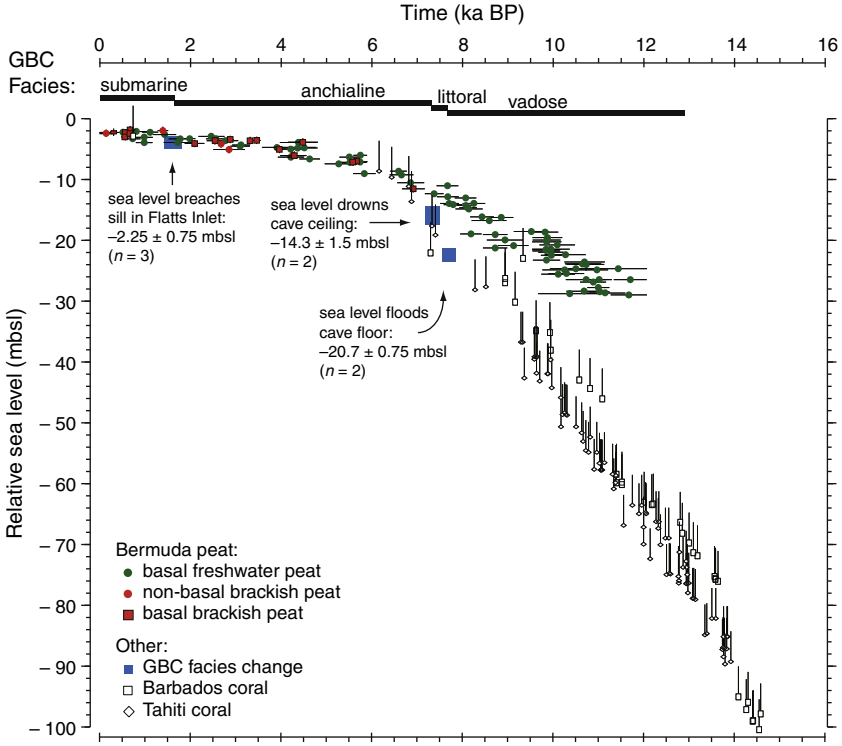

Fig. 9. Holocene sea level rise in Bermuda compared to coral sea-level index points at far-field sites (Bard et al., 1996; Peltier and Fairbanks, 2006; Bard et al., 2010). Bermuda basal brackish peat after this study (Appendix 1), Ellison (1993), Vollbrecht (1996), and Javaux (1999), which were verified with either brackish botanical remains or marsh foraminifera. Non-basal brackish peat data also denoted to be comprehensive, but these data may be impacted by peat autocompaction during sampling. No basal brackish peat dates older than 6.5 ka are yet regionally known. Vertical uncertainty on brackish peats corresponds to mean annual tide range (0.75 m) in Bermuda (Morris et al., 1977). Local freshwater peat data (green points) are often interpreted as the local sea-level curve, but these are maximum sea-level indicators only (Redfield, 1967; Neumann, 1971; Ashmore and Leatherman, 1984; Vollbrecht, 1996). The flooding history of GBC (blue squares) appears to closely follow the Holocene sea-level trends observed by Tahiti and Barbados corals.

littoral, anchialine, and submarine) can be observed in coastal karst basins, and they develop spatially variable lithofacies, from the cave entrance to interior, in response to eustacy. This concept is applied to the Holocene successions in Green Bay Cave (GBC).

6.1. GBC vadose facies

Based on estimates of sea level from areas least affected by ice sheets (far-field sites), sea level was located at approximately −65 mbsl at 12.9 ka (Bard et al., 1996; Siddall et al., 2003; Peltier and Fairbanks, 2006). Independent of these data, the recovered sedimentary evidence indicates that GBC was a vadose environment at 12.9 ka, with sea level located far below the cave floor at −21 mbsl, and thus the cave was in the vadose (unsaturated) zone above the paleo-water table (Fig. 9). The vadose facies in GBC is dominated by calcite rafts, which are unambiguously indicative of standing water in a cave (Taylor et al., 2004; Taylor and Chafetz, 2004; Kolesar and Riggs, 2007; Fornós et al., 2009). Standing water was likely intermittent and derived from transient dripwater pools, as indicated by a lack of aquatic microfossils and low sedimentation rate. The dry cave would have allowed *Poecilozonites* to crawl or wash into the cave, as observed in other Bermudian vadose cave facies (Hearty et al., 2004). Therefore, the timing of vadose facies deposition in GBC is consistent with the evidence for eustatic sea level being lower than the elevation of the cave floor (−20.7 mbsl), and GBC being a vadose environment at 12.9 ka.

6.2. GBC littoral facies

Sea-level rise flooded the floor of GBC to create a littoral cave environment at 7.7 ka, as evidenced from both calcite rafts and marine microfossils in the sediment (Table 3). Calcite rafts are speleothems, and speleothems are reputable sea-level indicators and index points (Harmon et al., 1981; Richards et al., 1994; Vesica et al., 2000). But, aquatic microfossils are needed to verify that the cave was actually flooded. The onset of calcite rafts in GBC provides a sea-level index point because their formation at a water table is nearly co-stratigraphic with sea level, assuming negligible effects from hydraulic head in the coastal zone (e.g., 5–10 mm km^{-1} in eastern Yucatan: Marin and Perry, 1994). A modern analog for these conditions occurs in Mallorca, Spain (Fig. 3), where calcite rafts are currently precipitating in littoral cave environments (Fornós et al., 2009). Occasional high-influx events of terrestrial organic matter (e.g., eolian, washover, hurricanes) likely caused the alternation between marine and terrestrial organic matter observed in core 5 (Fig. 7).

The presence of diverse microfossils indicates that a permanent marine ecosystem was present in the cave from 7.7 to 7.3 ka, thus validating that the calcite rafts are indicative of a water table. The Bermudian cave endemic ostracode *Paranesidea sterreri* and endemic gastropod *Caecum caverna* indicate that the microfossils are indicative of an in situ aquatic cave ecosystem, and were not merely transported into the cave from the lagoon. The fish bones in core 11 further suggest that a permanent marine ecosystem was present, but possible transport of these bones by bird predation cannot be ruled out. The benthic foraminifer *Spirophthalmidium emaciatum* is abundant only in Bermudian coastal caves (van Hengstum and Scott, 2011), which further supports the existence of a permanent marine ecosystem in the cave.

Based on the coeval calcite rafts and microfossils, the floor of GBC at -20.7 ± 0.3 m was definitively flooded by sea-level rise or by sea level 7.7 ka (Fig. 9). These results accord with all previously available maximum sea-level indicators from Bermuda (terrestrial peat). Modeled estimates of ice-loading effects in Bermuda from the Laurentide Ice Sheet project that relative sea level (RSL) during the Holocene was up to 5 m below the eustatic position, but this model has 4 to 8 m of vertical uncertainty in the mid-Holocene (Milne and Mitrovica, 2008). In contrast, the interpreted timing of when GBC flooded is consistent with the long-term trends of Holocene sea-level rise based on Tahiti and Barbados coral evidence (far-field sites, Fig. 9), when uncertainties with corals as sea-level proxies are considered (±5 m, Milne et al., 2009).

In the Grand Cayman (Caribbean), there is a prominent tidal notch at -18.5 ± 0.5 mbsl aged to ~7.6 ka. This tidal notch together with U-series ages on a local relict coral reef provides evidence for RSL at −19 mbsl at ~7.6 ka (Blanchon et al., 2002). These results are ~1.5 m above the elevation, and within age uncertainty, of when the sedimentary evidence indicates that sea level flooded the floor of GBC. Support for lower relative sea level in Bermuda at ~7.7 ka (−20.7 mbsl) compared to the Grand Cayman ~7.6 ka (−19 mbsl) is consistent with numerical models that indicate Bermuda was impacted by glacioisostatic adjustment, but the magnitude of this adjustment appears quite less than the current modeled estimates (Milne and Mitrovica, 2008). However, a definitive understanding of the deglacial adjustment of the Bermuda platform will require a larger dataset. Because GBC sea level index points are in general agreement with other global evidence, stratigraphy in coastal karst basins represents an innovative new source of sea-level information on carbonate platforms.

6.3. GBC anchialine facies

Deposition of the anchialine facies began as sea-level rise drowned the cave ceiling and created an entirely phreatic cave. When groundwater reached the cave ceiling, the prerequisite conditions for calcite raft formation no longer existed, ceasing their precipitation and accumulation in the cave sediment record. Based on the lithologic transition in cores 5 and 9, this threshold was reached at ~7.3 ka ago when sea level drowned the cave ceiling, elevated at -14.3 ± 1.5 mbsl. There is larger uncertainty on this elevation because caves ceilings are not a flat surface, but this still provides another sea-level index point at ~7.3 ka.

The anchialine facies in GBC consists of the diamict and slackwater lithofacies, which are intercalated and dominated by terrestrial sediments (Table 3). Haphazard sediment fluxes generate cave diamicts, such as fluvial mass entrainment and re-deposition of cave sediment or entrance deposits. In contrast, slackwater lithofacies accumulate at a distance from cave entrances as clay and silt settle out of suspension (Ford and Williams, 1989; Bosch and White, 2007; White, 2007).

Modern diamict occurs in GBC from Cliff Pool Sinkhole down into the cave, and comprises sandy carbonate sediment, terrestrial remains (plants and animal bones), and aquatic debris (bivalve shells, algae; van Hengstum and Scott, 2011). These coarse-grained sediments are deposited as bed load, whereas the finer-grained sediments are transported into the cave as suspended load and form slackwater lithofacies (tops of cores 1 and 8) before pinching out into carbonate mud (top of core 10, Fig. 8). These modern patterns are consistent with downcore observations. Coeval diamict lithofacies in the different cores has attenuating PSDs with increasing distance into the cave. For example, core 1 is predominantly sandy, whereas cores 8 and 10 are silty-sand at approximately time-equivalent horizons, and the slackwater lithofacies laterally pinches-out between cores 9, 12, and 11 (Fig. 8).

The condensed and expanded horizons in the GBC anchialine facies indicate variable sedimentation rates. Variable sedimentation rates were also observed in the anchialine facies in Aktun Ha Cave, Mexico, from erosion related to storminess or climate-forced precipitation changes that were confounded by changing groundwater flow rates (van Hengstum et al., 2010). In contrast, continuous late Holocene sedimentation characterizes the anchialine facies in Yax Chen Cave (Mexico) because a local mangrove system provided a constant sediment supply (Gabriel, 2009). Because a constant source of

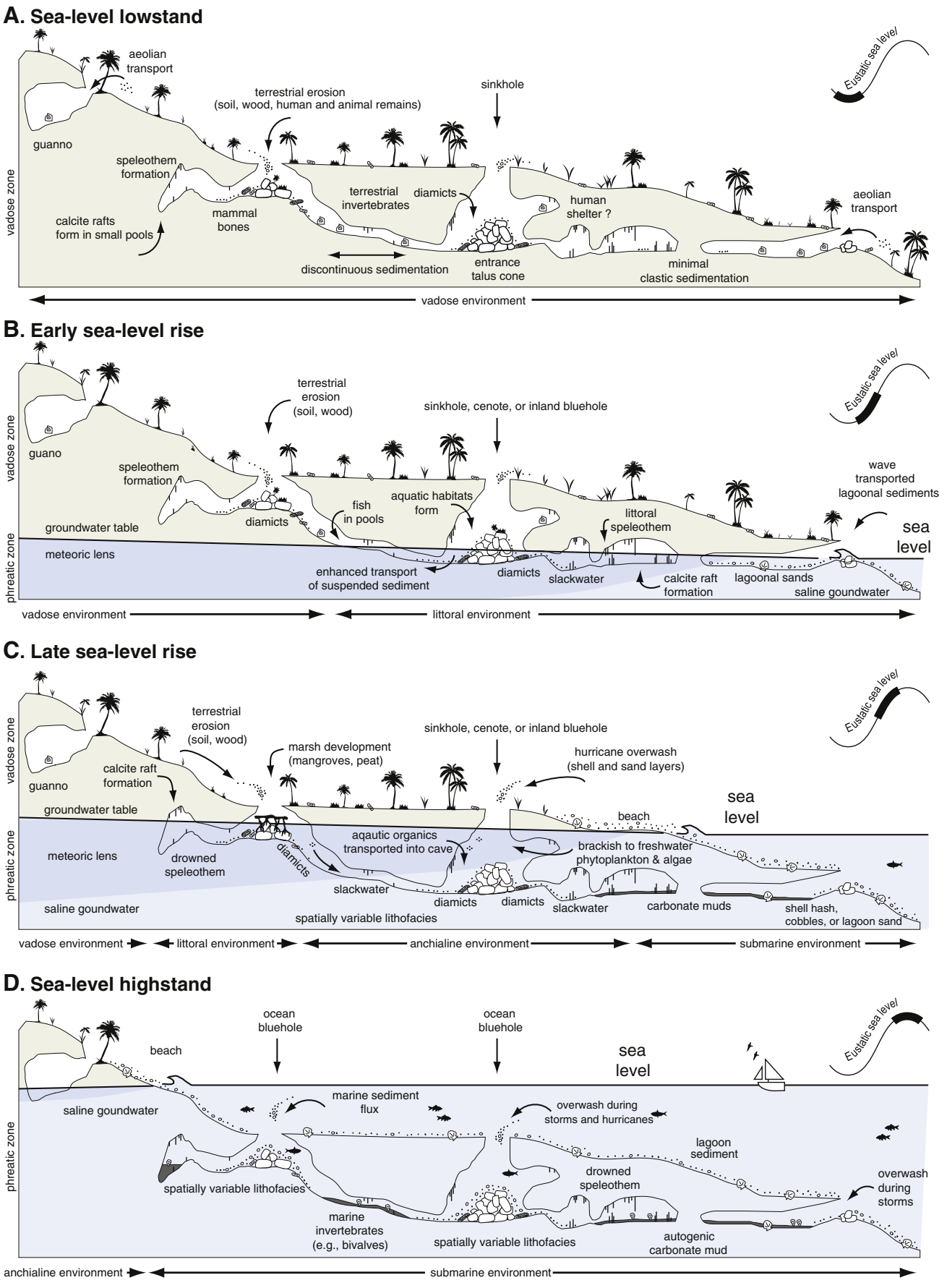

Fig. 10. A conceptual model depicting environmental development and sedimentation patterns in coastal karst basins during sea-level rise.

sediment is lacking in GBC, the anchialine facies appears most sensitive to terrestrial erosion products entering Cliff Pool Sinkhole.

6.4. GBC submarine facies

Sea-level rise may eventually cause saline groundwater or the ocean to completely flood coastal karst basins to create submarine environments. Saline groundwater definitively flooded GBC at 1.6 ka based on the onset of the carbonate mud lithofacies. In open-ocean lagoons, carbonate mud is deposited as eustatic sea-level rise floods a lagoon and initiates oceanic circulation (Gischler, 2003; Zinke et al., 2005). Modern coastal circulation between Harrington Sound and the ocean off Bermuda occurred recently when the sill in Flatt's Inlet (-2.25 m $\pm$ 0.5 mbsl) was breached by Holocene sea-level rise (Vollbrecht, 1996). Sea level breaching a sill 2 to 3 mbsl at 1.6 ka is within uncertainty of Holocene sea-level rise in Bermuda (Fig. 9; Ellison, 1993; Javaux, 1999), and would have caused open circulation between Harrington Sound, the ocean, and GBC; and initiated modern saline groundwater circulation in GBC. Thus, sea-level rise forced GBC to transition from an anchialine to submarine environment at 1.6 ka, and caused the anchialine facies to become restricted to the area near the base of Cliff Pool Sinkhole (Fig. 8). Although the entire cave became marine, the base of Cliff Pool Sinkhole area remains an anchialine environment because it receives a constant flux of terrestrial sediment that primarily controls the local environmental conditions (van Hengstum and Scott, 2011). This is evidenced by the marine microfossils in the topmost slackwater lithofacies in cores 1 and 8, as previously discussed, and the modern assemblage of anchialine cave foraminifera living there (van Hengstum and Scott, 2011).

The submarine facies consists of the carbonate mud and shell hash lithofacies, and the submarine biofacies colonized at 1.6 ka; comprising brachiopods, *Barbatia domingensis*, corals, and marine foraminifera (Table 3). *Barbatia domingensis* is a sessile suspension feeder ubiquitous in Bermudian caves, more commonly found attached to coral and reef cavities in Florida, Bermuda and Bonaire (Bretzsky, 1967; Choi and Ginsburg, 1983; Logan et al., 1984; Koblunk and Lysenko, 1986; Zinke et al., 2005). Corallites of *Coenocyathus goreaui* are also present, which is a cave-adapted Bermudian coral (Cairns, 2000). These organisms collectively indicate that a circulated marine habitat was initiated in GBC at 1.6 ka, characterizing the newly formed submarine cave environment.

The sand horizons below 10 cm in core 3 (Figs. 6, 8) and the articulated bivalve horizon in core 6 (Fig. 8) suggest that the cave entrance was affected by external events. The sand horizons indicated by the PSDs in core 3 probably relate to storm or hurricane activity, causing increased turbulence in the cave entrance from the inward transport of lagoonal sediments. The imbricated, monospecific, articulated bivalves in core 6 (~0.7 ka), however, may be suggestive of an Atlantic tsunami event because similar articulated bivalve horizons have been used as a tsunamite proxy in the Mediterranean and Indian Oceans (Donato et al., 2008). However, a more extensive survey is needed to assess the distribution of this shell horizon to be conclusive on its origin.

7. Sea level controls coastal karst basins worldwide

The latest Pleistocene to Holocene succession from GBC indicates that glacioeustacy controls environmental and sedimentary development in coastal karst basins (Fig. 10). Conceptually, spatially variable sedimentary processes cause a vadose facies to develop during a lowstand, which become interrupted by permanent aquatic processes as sea level floods a carbonate platform and causes littoral cave environments develop. As sea level and groundwater continue to rise in synchrony and drown cave passages, anchialine environments develop that will eventually become submarine environments in a completely highstand scenario.

The *vadose facies* develops in coastal karst basins in the unsaturated vadose zone that are currently vadose environments (Fig. 10A). Spatially variable processes will give rise to spatially diverse lithofacies, such as guano deposits, calcite rafts, or entrance talus (Gospodarič, 1988; Ford and Williams, 1989; Woodward and Goldberg, 2001; Gilbertson et al., 2005; White, 2007). Vadose cave sediments have arguably received the most research attention, but their units are rarely considered part of a broader facies assemblage in the literature. Woodward and Goldberg (2001) summarized many physical processes that influence what we envisage as the vadose facies, which is often overprinted by pedogenic processes. Vadose deposits often preserve paleoecological and paleoclimate records (Hearty et al., 2004; Panno et al., 2004; Polk et al., 2007; Wurster et al., 2008; Hearty and Olson, 2010), so the research value of vadose cave sediments is well understood. However, the advance presented here is that all the deposits that develop in the vadose zone can be attributed to a vadose facies, which then may be investigated in a context of sea-level rise.

Littoral environments develop in coastal karst basins when they become inundated by groundwater in response to sea-level rise (Fig. 10B). Flooding creates permanent standing water in the cave, resulting in new physical processes, aquatic ecosystems, and new deposits that can be collectively attributed to a *littoral facies*. Littoral cave environments that open into lagoons are influenced by waves that can transport lagoonal sediments inward, such as in Castle Grotto, Bermuda, and Blue Marino Cave, Italy (Corriero et al., 2001). Littoral environments may also be connected to a sinkhole that enables terrestrial sediments to erode into caves, whereas calm conditions in distal caves may allow for calcite raft deposition (Fornós et al., 2009). In summary, at least four factors influence the littoral facies: coastal position, basin geomorphology, hydrodynamics, and water source (groundwater versus ocean). As such, the littoral facies comprises sediments from terrestrial, aquatic, or speleogenic origins (e.g., calcite rafts).

Cave sediments can now be used in sea-level research because the littoral facies provides a sea-level indicator after the uncertainties imparted by hydraulic gradients are considered. Overall, the strata in GBC are analogous to transgressive sequences in lagoons (Gischler, 2003; Zinke et al., 2005). Instead of the basal palesols and *Rhizophora* peats observed in lagoons, however, GBC has a basal calcite raft lithofacies (vadose facies) followed by calcite rafts and mud lithofacies (littoral facies). In a subaerial sinkhole, Gabriel et al. (2009) recovered a *Rhizophora* peat lithofacies in the central cenote of Aktun Ha Cave caused by sea-level flooding the Yucatan platform (Mexico). In a Pleistocene example, littoral cave deposits in elevated Bermudian caves at $+21$ m were attributed to a similar position of sea level during Marine Isotope Stage 11 (Olson and Hearty, 2009; van Hengstum et al., 2009b).

Sea-level change also impacts cave ecosystems and this can be preserved in the fossil record. For example, sea-level rise changed habitat availability for monk seal populations in Bel Torrente Cave (Sardinia, Italy). Based on a comparison with the conceptual model presented here, the cave evolved from a littoral to an anchialine environment after ~10 m of sea-level rise over the last ~6.5 ka. As a result, skeletal remains indicate that the cave is no longer a suitable calving ground for monk seals (De Waele et al., 2009).

Anchialine environments develop in coastal karst basins that are completely flooded and dominated by terrestrial processes, which in turn cause *anchialine facies* to develop (Fig. 10C). In GBC, a coarser grained diamict lithofacies at the anchialine cave entrances passes into fine-grained slackwater lithofacies in the distal cave. This sedimentation pattern was also observed in Aktun Ha Cave, Mexico, which was used by van Hengstum et al. (2010) to reconstructed local hydrogeologic changes over the mid- to late-Holocene. Elsewhere, Alverez Zarikian et al. (2005) used ostracode paleoecology and $\delta^{18}O_{carb}$ in an anchialine facies to reconstruct long-term paleohydrogeological and paleoclimate changes in a sediment core recovered from Little Salt Spring (Florida). Lastly, Steadman et al. (2007) used mid- to late-Holocene anchialine

entrance diamicts from Sawmill Sink (Abaco, Bahamas) to reconstruct local paleoecology. In contrast, sedimentary deposits located deeper into Sawmill Sink from a Pleistocene owl roost can be attributed to a prior vadose lithofacies, perhaps aged to the last glacial maximum when lower sea levels promoted suitable nesting grounds in the cave (Steadman et al., 2007). Based on the available evidence, similar sedimentary processes operate globally in anchialine environments too.

Eventually, sea-level rise completely floods a karst platform and submarine cave environments are created. The few examples of sediments attributable to a *submarine facies* have similar lithofacies to GBC, which developed in response to circulating seawater (Fig. 10D). In Japan, a 7000-year paleoceanographic record of the East China Sea was obtained from Daidokutsu Cave, a tidally-influenced submarine cave located on a fore reef slope (Kitamura et al., 2007; Omori et al., 2010; Yamamoto et al., 2010). A coarse-grained lithofacies characterizes the entrance to Daidokutsu Cave, which attenuates into carbonate mud in the cave interior, similar to GBC (see Fig. 2 in Omori et al., 2010). Ocean blueholes arguably represent the final developmental phase when sea-level completely drowns karst platforms and coastal karst basins (Mylroie et al., 1995a; Shinn et al., 1996). This state is exemplified by Blue Hole, Belize, wherein the sedimentation is controlled by background productivity and storm transport of coastal sediments (Gischler et al., 2008). As with all the other facies discussed, a similar global pattern of sedimentation emerges for submarine environments when modern and core records are considered collectively.

8. Conclusions

Green Bay Cave (GBC), Bermuda, affords the first succession from a coastal karst basin that spans the Holocene. Six lithofacies were recovered in upward succession that can be organized into four sedimentary depositional environments: vadose, littoral, anchialine, and submarine. The timing of facies changes is closely related to Holocene sea-level rise in Bermuda, which systematically forced environmental change in GBC. Vadose conditions existed in GBC from 12.9 ka until the ocean flooded the cave floor at ~7.7 ka to create a littoral cave environment. This promoted coeval calcite raft precipitation (water table proxy) and a permanent marine ecosystem supporting a diverse microfauna. Concurrently rising sea and groundwater levels eventually drowned the ceiling of GBC at 7.3 ka, which transitioned the cave into an anchialine cave environment dominated by terrestrial sedimentation and allowed a brackish meteoric lens to develop. Finally, Holocene sea-level rise breeched a local sill at 1.6 ka and caused open oceanic circulation between Harrington Sound, the ocean, causing the final transition of GBC into a submarine cave environment. These results indicate that glacioeustacy exerts a fundamental control on sedimentary and environmental development in coastal karst basins. The successions from GBC are the first to document a complete Holocene facies succession, but available sedimentary evidence from other coastal karst basins in Florida, the Bahamas, Japan, Belize, Mexico, and the Mediterranean all accord with the facies model presented here. Inherited geomorphology and coastal position, however, will likely remain important factors influencing the lateral accretion, spatial variability, and vertical development of lithofacies in coastal karst basins.

Supplementary materials related to this article can be found online at doi:10.1016/j.margeo.2011.05.004

Acknowledgments

This research was only possible with the generous support in Bermuda from the Bermuda Cavers Group (Bruce Williams, Gil Nolan, Leon Kemp, and Paul Larrett) and the Tucker family. Stephen Cairns (coral) and David Johnson (fish bones) are thanked for assisting with identifying fossil remains, as well as technical support from Taryn Gray and Shawna Little. All samples were collected in accordance with a permit from the Bermuda Department of Environmental Protection (SP081103). Insightful comments from Martin Gibling, John Pohlman, and an anonymous reviewer are thanked for improving an earlier version of this manuscript.

The inaugural Johanna M. Resig Fellowship from the Cushman Foundation for Foraminiferal Research and an *NSERC* Alexander Graham Bell Canada Graduate Scholarship to PvH provided primary research support, along with student research grants from the Geologic Society of America, the Cave Research Foundation, Bermuda Zoological Society, and the Sigma Xi Scientific Research Society.

References

Airoldi, L., Cinelli, F., 1996. Variability of fluxes of particulate material in a submarine cave with chemolithoautotrophic inputs of organic carbon. Marine Ecology Progress Series 139, 205–217.
Alverez Zarikian, C.A., Swart, P.K., Gifford, J.A., Blackwelder, P.L., 2005. Holocene paleohydrology of Little Salt Spring, Florida, based on ostracod assemblages and stable isotopes. Palaeogeography, Palaeoclimatology, Palaeoecology 225, 134–156.
Ashmore, S., Leatherman, S.P., 1984. Holocene sedimentation in Port Royal Bay, Bermuda. Marine Geology 56, 289–298.
Bard, E., Hamelin, B., Arnold, M., Montaggioni, L., Cabioch, G., Faure, G., Rougerie, F., 1996. Deglacial sea-level record from Tahiti corals and the timing of global meltwater discharge. Nature 382, 241–244.
Bard, E., Hamelin, B., Delanghe-Sabatier, D., 2010. Deglacial meltwater pulse 1B and Younger Dryas sea levels revisted with boreholes at Tahiti. Science 327, 1235–1237.
Beierle, B.D., F., L.S., Cockburn, J.M.H., Spooner, I., 2002. A new method for visualizing sediment particle size distribution. Journal of Paleolimnology 27 (279–283).
Blanchon, P., Jones, B., Ford, D.C., 2002. Discovery of a submerged relic reef and shoreline off Grand Cayman: further support for an early Holocene jump in sea level. Sedimentary Geology 147, 253–270.
Bosch, R.F., White, W.B., 2007. Lithofacies and transport of clastic sediments in karstic aquifers. In: Sasowsky, I.D., Mylroie, J. (Eds.), Studies of Cave Sediments: Physical and Chemical Records of Paleoclimate. Springer, pp. 1–22.
Bowen, D.Q., 2010. Sea level 400 000 years ago (MIS 11): analogue for present and future sea-level? Climate of the Past 6, 19–29.
Bretz, J.H., 1960. Bermuda: a partially drowned, late mature, Pleistocene karst. Geological Society of America Bulletin 71, 1729–1754.
Bretzsky, S.S., 1967. Environmental factors influencing the distribution of *Barbatia domingensis* (mollusca, bivalvia) on the Bermuda Platform. Postilla 108, 1–14.
Cairns, S.D., 2000. A revision of the shallow-water Azooxanthellate scleractinia of the western Atlantic. Studies on the Natural History of the Caribbean Region 75, 1–208.
Cate, J.R., 2009. Assessing the Impact of Groundwater Pollution from Marine Caves on Nearshore Seagrass Beds in Bermuda. Masters Thesis, Texas A&M, Galveston. 101 pp.
Choi, D.R., Ginsburg, R.N., 1983. Distribution of coelobites (cavity-dwellers) in coral rubble across the Florida reef tract. Coral Reefs 2 (3), 165–172.
Corriero, G., Liaci, L.S., Ruggiero, D., Pansini, M., 2001. The sponge community of a semi-submerged Mediterranean Cave. Marine Ecology Progress Series 21 (1), 85–96.
De Waele, J., Brook, G.A., Oertel, A., 2009. Monk seal (Monachus monachus) bones in Bel Torrente Cave (Central-east Sardinia) and their paleogeographical significance. Journal of Cave and Karst Studies 71 (1), 16–23.
Donato, S.V., Reinhardt, E.G., Boyce, J.I., Rothaus, R., Vosmer, T., 2008. Identifying tsunami deposits using bivalve shell taphonomy. Geology 36 (3), 199–202.
Donato, S.V., Reinhardt, E.G., Boyce, J.I., Pilarczyk, J.E., Jupp, B.P., 2009. Particle-size distribution of inferred tsunami deposits in Sur Lagoon, Sultanate of Oman. Marine Geology 257 (1–4), 54–64.
Donnelly, J.P., Woodruff, J.D., 2007. Intense hurricane activity over the past 5,000 years controlled by El Niño and the West African Monsoon. Nature 447, 465–468.
Dorale, J.A., Onac, B.P., Fornós, J.J., Ginés, J., Ginés, A., Tuccimei, P., Peate, D.W., 2010. Sea-level highstand 81,000 years ago in Mallorca. Science 327, 860–863.
Druffel, E.R.M., 1997. Pulses of rapid ventilation in the North Atlantic surface ocean during the past century. Science 275, 1454–1457.
Dutton, A., Bard, E., Antonioli, F., Esat, T.M., Lambeck, K., McCulloch, M.T., 2009. Phasing and amplitude of sea-level and climate change during the penultimate interglacial. Nature Geoscience 2, 355–359.
Ellison, J.C., 1993. Mangrove retreat with rising sea level, Bermuda. Estuarine, Coastal, and Shelf Science 37, 75–87.
Enos, P., Sawatsky, L.H., 2003. Pore networks in Holocene carbonate sediments. Journal of Sedimentary Petrology 51, 961–985.
Fichez, R., 1990. Decrease in allochthonous organic inputs in dark submarine caves, connection with lowering in benthic community richness. Hydrobiologia 207, 61–69.
Florea, L.J., Vacher, H.L., Donahue, B., Naar, D., 2007. Quaternary cave levels in peninsular Florida. Quaternary Science Reviews 26, 1344–1361.
Ford, D., Williams, P., 1989. Karst Geomorphology and Hydrology. Unwin Hyman, London.
Fornós, J.J., Ginés, J., Gràcia, F., 2009. Present-day sedimentary facies in the coastal karst caves of Mallorca island (western Mediterranean). Journal of Cave and Karst Studies 71 (1), 86–99.
Gabriel, J.J., 2009. Late Holocene (3500 yBP) salinity changes and their climatic implications as recorded in an anchialine cave system, Ox Bel Ha, Yucatan, Mexico. MSc Thesis, McMaster University.

Gabriel, J.J., Reinhardt, E.G., Peros, M.C., Davidson, D.E., van Hengstum, P.J., Beddows, P.A., 2009. Palaeoenvironmental evolution of Cenote Aktun Ha (Carwash) on the Yucatan Peninsula, Mexico and its response to Holocene sea-level rise. Journal of Paleolimnology 42 (2), 199–213.
Gilbertson, D., Bird, M., Hunt, C., McLaren, S., Pyatt, B., Rose, J., Stephens, M., 2005. Past human activity and geomorphological change in a guano-rich tropical cave mouth: the late Quaternary succession in the Great Cave Niah, Sarawak. Asian Perspectives 44 (1), 16–41.
Ginés, A., Ginés, J., 2007. Eogenetic karst, glacioeustatic cave pools and anchialine environments on Mallorca Island. International Journal of Speleology 36 (2), 57–67.
Gischler, E., 2003. Holocene lagoonal development in the isolated carbonate platforms off Belize. Sedimentary Geology 159 (1–2), 113–132.
Gischler, E., Shinn, E.A., Oschmann, W., Fiebig, J., Buster, N.A., 2008. A 1500-year Holocene Caribbean climate archive from the Blue Hole, Lighthouse Reef, Belize. Journal of Coastal Research 24 (6), 1495–1505.
Gospodarič, R., 1988. Paleoclimatic record of cave sediments from Postojna karst. Annales de la Société Géologique de Belgique 111 (91–95).
Guillem, J., 2007. Tafonomía, taxonomía y ecología de los foraminíferos de la albufera de Torreblanca. PhD Thesis, Universitat de València, 523 p. www.tdx.cbuc.es.
Harmon, R.S., Land, L.S., Mitterer, R.M., Garett, P., Schwarcz, H.P., Larson, G.J., 1981. Bermuda sea level during the last interglacial. Nature 289, 481–483.
Hearty, P.J., Olson, S.L., 2010. Geochronology, biostratigraphy, and changing shell morphology in the land snail subgenus Poecilozonites during the Quaternary of Bermuda. Palaeogeography, Palaeoclimatology, Palaeoecology 293 (1–2), 9–29.
Hearty, P.J., Kindler, P., Cheng, H., Edwards, R.L., 1999. Evidence for a +20 m middle Pleistocene sea-level highstand (Bermuda and Bahamas) and partial collapse of Antarctic ice. Geology 27, 375–378.
Hearty, P.J., Olson, S.L., Kaufman, D.S., Edwards, R.L., Cheng, H., 2004. Stratigraphy and geochronology of pitfall accumulations in caves and fissures, Bermuda. Quaternary Science Reviews 23, 1151–1171.
Heiri, O., Lotter, A.F., Lemcke, G., 2001. Loss on ignition as a method for estimating organic and carbonate content in sediments: reproducibility and comparability of results. Journal of Paleolimnology 25, 101–110.
Holthuis, L.B., 1973. Caridean shrimps found in land-locked saltwater pools at four Indo-west Pacific localities (Sinai peninsula, Funafuti atoll, Maui and Hawaii islands), with the description of the new genus and four new species. Zoologishe Verhandelingen 128, 1–48.
Javaux, E., 1999. Benthic Foraminifera from the Modern Sediments of Bermuda: Implications for Holocene Sea-level Studies. Dalhousie University. 625 pp.
Kemp, A.C., Vane, C.H., Horton, B.P., Culver, S.J., 2010. Stable carbon isotopes as potential sea-level indicators in salt marshes, North Carolina, USA. The Holocene 20 (4), 623–636.
Kitamura, A., Yamamoto, N., Kase, T., Ohashi, S., Hiramoto, M., Fukusawa, H., Watanabe, T., Irino, T., Kojitani, H., Shimamura, M., Kawakami, I., 2007. Potential of submarine-cave sediments and oxygen isotope composition of cavernicolous micro-bivalve as a late Holocene paleoenvironmental record. Global and Planetary Change 55 (4), 301–316.
Koblunk, D.R., Lysenko, M.A., 1986. Reef-dwelling molluscs in open framework cavities Bonaire, N.A., and their potential for preservation in a fossil reef. Bulletin of Marine Science 39 (3), 656–672.
Kolesar, P.T., Riggs, A.C., 2007. Influence of depositional environmental on Devil's Hole Calcite morphology and petrology. In: Sasowsky, I.D., Mylroie, J. (Eds.), Studies of Cave Sediments: Physical and Chemical Records of Paleoclimate. Springer, pp. 227–241.
Lamb, A.L., Wilson, G.P., Leng, M.J., 2006. A review of coastal paleoclimate and relative sea-level reconstructions using δ13C and C/N ratios in organic material. Earth Science Reviews 75, 29–57.
Land, L.S., Mackenzie, F.T., Gould, S.J., 1967. The Pleistocene history of Bermuda. GSA Bulletin 78, 993–1006.
Logan, A., Mathers, S.M., Thomas, M.L.H., 1984. Sessile invertebrate coelobite communities from reefs of Bermuda: species composition and distribution. Coral Reefs 2, 205–213.
Maddocks, R.F., Iliffe, T.M., 1986. Podocopid ostracoda of Bermudian caves. Stygologia 2 (1/2), 26–76.
Marin, L.E., Perry, E.C., 1994. The hydrogeology and contaminant potential of northwestern Yucatan, Mexico. Geofis International 33, 619–623.
Medina-Elizalde, M., Burns, S.J., Lea, D.W., Asmerom, Y., von Gunten, L., Polyak, V., Vuille, M., Karmalkara, A., 2010. High resolution stalagmite climate record from the Yucatán Peninsula spanning the Maya terminal classic period. Earth and Planetary Science Letters 298, 255–262.
Milne, G.A., Mitrovica, J.X., 2008. Searching for eustacy in deglacial sea-level histories. Quaternary Science Reviews 27, 2292–2302.
Milne, G.A., Gehrels, W.R., Hughes, C.W., Tamisiea, M.E., 2009. Identifying the causes of sea-level change. Nature Geoscience 2, 471–478.
Moolenbeek, R.G., Faber, M.J., Iliffe, T.M., 1988. Two new species of the genus Caecum (gastropoda) from marine caves on Bermuda. Studies in Honour of Dr. Pieter Wagenaar Hummelinck, 123, pp. 209–216.
Morris, B., Barnes, J., Brown, F., Markham, J., 1977. The Bermuda Marine Environment: A Report of the BERMUDA Inshore Waters Investigations 1976–1977. Bermuda Biological Station Special Publication, 17. Bermuda Biological Station for Research, St. Georges, Bermuda, 120 pp.
Mylroie, J.E., 2008. Late Quaternary sea-level position: evidence from Bahamian carbonate deposition and dissolution cycles. Quaternary International 183 (1), 61–75.
Mylroie, J.E., Carew, J.L., 1988. Solution conduits as indicators of late Quaternary sea level position. Quaternary Science Reviews 7 (1), 55–64.
Mylroie, J.E., Carew, J.L., 1990. The flank margin model for dissolution cave development in carbonate platforms. Earth Surface Process Landforms 15 (5), 413–424.
Mylroie, J.R., Mylroie, J.E., 2007. Development of the carbonate island karst model. Journal of Cave and Karst Studies 69 (1), 59–75.
Mylroie, J.E., Carew, J.L., Moore, A.I., 1995a. Blue holes: definitions and genesis. Carbonates and Evaporites 10 (2), 225–233.
Mylroie, J.E., Carew, J.L., Vacher, H.L., 1995b. Karst development in the Bahamas and Bermuda. In: Curran, H.A., White, B. (Eds.), Terrestrial and Shallow Marine Geology of the Bahamas and Bermuda: Geological Society of America Special Paper, 300, pp. 251–267.
Neumann, A.C., 1971. Quaternary sea-level data from Bermuda. Quaternaria 14, 41–43.
Ogrinc, N., Fontolan, G., Faganeli, J., Covelli, S., 2005. Carbon and nitrogen isotope compositions of organic matter in coastal marine sediments (the Gulf of Trieste, N Adriatic Sea): indicators of sources and preservation. Marine Chemistry 95, 163–181.
Olson, S.L., Hearty, P.J., 2009. A sustained +21 m sea-level highstand during MIS 11 (400 ka): direct fossil and sedimentary evidence from Bermuda. Quaternary Science Reviews 28, 271–285.
Omori, A., Kitamura, A., Fujita, K., Honda, K., Yamamoto, N., 2010. Reconstruction of light conditions within a submarine cave during the past 7000 years based on the temporal and spatial distribution of algal symbiont-bearing large benthic foraminifers. Palaeogeography, Palaeoclimatology, Palaeoecology 292, 443–452.
Palmer, A.N., Palmer, M.V., Queen, J.M., 1977. Geology and origin of the caves of Bermuda. Proceedings of the Seventh International Congress of Speleology, Sheffield, pp. 336–339.
Panno, S.V., Curry, B.B., Wang, H., Hackley, K.C., Liu, C., Lundstrom, C., Zhou, J., 2004. Climate change in southern Illinois, USA, based on the age and δ13C of organic matter in cave sediments. Quaternary Research 61, 301–313.
Peltier, W.R., Fairbanks, R.G., 2006. Global glacial ice volume and Last Glacial Maximum duration from an extended Barbados sea level record. Quaternary Science Reviews 25 (23–24), 3322–3337.
Pohlman, J.W., Iliffe, T.M., Cifuentes, L.A., 1997. A stable isotope study of organic cycling and the ecology of an anchialine cave ecosystem. Marine Ecology Progress Series 155, 17–27.
Polk, J.S., van Beynen, P.E., Reeder, P.P., 2007. Late Holocene environmental reconstruction using cave sediments from Belize. Quaternary Research 68, 53–63.
Redfield, A.C., 1967. Postglacial change in sea level in the western North Atlantic Ocean. Science 157 (3787), 687–691.
Reimer, P.J., Baillie, M.G.L., Bard, E., Bayliss, A., Beck, J.W., Blackwell, P.G., Ramsey, C.B., Buck, C.E., Burr, G.S., Edwards, R.L., Freidrich, M., Groots, P.M., Guilderson, T.P., Hajdas, I., Heaton, T.J., Hogg, A.G., Hughen, K.A., Kaiser, K.F., Kromer, B., McCormac, F.G., Manning, S.W., Reimer, R.W., Richards, D.A., Southon, J.R., Talamo, S., Turney, C.S.M., van der Plicht, J., Weyhenmeyer, C.E., 2009. IntCal09 and Marine09 radiocarbon age calibration curves, 0–50,000 years Cal BP. Radiocarbon 51 (4), 1111–1150.
Richards, D.A., Smart, P.L., Edwards, R.L., 1994. Maximum sea levels for the last glacial period from U-series ages of submerged speleothems. Nature 367, 357–360.
Sánchez, S.O., Alcocer, J., Escobar, E., Lugo, A., 2002. Phytoplankton of cenotes and anchialine caves along a distance gradient from the northeastern coast of Quintana Roo, Yucatan Peninsula. Hydrobiologia 467, 79–89.
Schmitter-Soto, J.J., Comín, F.A., Escobar-Briones, E., Herrera-Silveira, J., Alcocer, J., Suárez-Morales, E., Elías-Gutiérrez, M., Día-Arce, V., Marín, L.E., Steinich, B., 2002. Hydrogeochemical and biological characteristics of cenotes in the Yucatan Peninsula (SE Mexico). Hydrobiologia 467, 215–228.
Shinn, E.A., Reich, C.D., Locker, S.D., Hine, A.C., 1996. A giant sediment trap in the Florida Keys. Journal of Coastal Research 12 (4), 953–959.
Siddall, M., Rohling, E.J., Almogi-Labin, A., Hemleben, C., Meischner, D., Schmelzer, I., Smeed, D.A., 2003. Sea-level fluctuations during the last glacial cycle. Nature 423, 853–858.
Steadman, D.W., Franz, R., Morgan, G.S., Albury, N.A., Kakuk, B., Broad, K., Franz, S.E., Tinker, K., Pateman, M.P., Lott, T.A., Jarzen, D.M., Dilcher, D.L., 2007. Exceptionally well preserved late Quaternary plant and vertebrate fossils from a blue hole on Abaco, the Bahamas. Proceedings of the National Academy of Sciences 104 (50), 19897–19902.
Stock, J.H., Iliffe, T.M., Williams, D., 1986. The concept "anchialine" reconsidered. Stygologia 2 (1/2), 90–92.
Surić, M., Juračić, M., Horvatinčić, N., Bronić, I.K., 2005. Late-Pleistocene–Holocene sea-level rise and the pattern of coastal karst inundataion: records from submerged speleothems alon the Eastern Adriatic Coast (Croatia). Marine Geology 214, 163–175.
Taylor, P.M., Chafetz, H.S., 2004. Floating rafts of calcite crystals in cave pools, central Texas, U.S.A.: crystal habit vs. saturation state. Journal of Sedimentary Research 74 (3), 328–341.
Taylor, M.P., Drysdale, R.N., Carthew, K.D., 2004. The formation and environmental significance of calcite rafts in tropical tufa-depositing rivers in northern Australia. Sedimentology 51, 1089–1101.
Teeter, J.W., 1995. Holocene saline lake history, San Salvador Island, Bahamas. In: Curan, H.A., White, B. (Eds.), Terrestrial and Shallow Marine Geology of the Bahamas and Bermuda: Geological Society of America Special Paper, 300, pp. 117–124.
Thornton, S.F., McManus, J., 1994. Application of organic carbon and nitrogen stable isotopes and C/N ratios as source indicators of organic matter provenance in estuarine systems: evidence from the Tay Estuary, Scotland. Estuarine, Coastal and Shelf Science 38 (3), 219–233.
Vacher, H.L., Hearty, P.J., 1989. History of stage 5 sea level in Bermuda: review with new evidence of a brief rise to present sea level during substage 5a. Quaternary Science Reviews 8, 159–168.

Vacher, H.L., Rowe, M.P., 1997. Geology and hydrogeology of Bermuda. In: Vacher, H.L., Quinn, T.M. (Eds.), Geology and Hydrogeology of Carbonate Islands: Developments in Sedimentology, 54. Elsevier, Amsterdam, pp. 35–90.

Vacher, H.L., Rowe, M.P., Garrett, P., 1989. The Geological Map of Bermuda. The Ministry of Works and Engineering, Hamilton, Bermuda.

Vacher, H.L., Hearty, P.J., Rowe, M.P., 1995. Stratigraphy of Bermuda: nomenclature, concepts, and status of multiple systems of classification. In: Curran, H.A., White, B. (Eds.), Terrestrial and Shallow Marine Geology of the Bahamas and Bermuda: Geological Society of America Special Paper, 300, pp. 271–294.

van Hengstum, P.J., Scott, D.B., 2011. Ecology of foraminifera and habitat variability in an underwater cave: distinguishing anchialine versus submarine cave environments. Journal of Foraminiferal Research 41 (3), 201–229.

van Hengstum, P.J., Reinhardt, E.G., Boyce, J.I., Clark, C., 2007. Changing sedimentation patterns due to historical land-use change in Frenchman's Bay, Pickering, Canada: evidence from high-resolution textural analysis. Journal of Paleolimnology 37, 603–618.

van Hengstum, P.J., Reinhardt, E.G., Beddows, P.A., Schwarcz, H.P., Garbriel, J.J., 2009a. Foraminifera and testate amoebae (thecamoebians) in an anchialine cave: surface distributions from Aktun Ha (Carwash) cave system, Mexico. Limnology and Oceanography 54 (1), 391–396.

van Hengstum, P.J., Scott, D.B., Javaux, J.J., 2009b. Foraminifera in elevated Bermudian caves provide further evidence for +21 m eustatic sea level during marine isotope stage 11. Quaternary Science Reviews 28, 1850–1860.

van Hengstum, P.J., Reinhardt, E.G., Beddows, P.A., Gabriel, J.J., 2010. Investigating linkages between Holocene paleoclimate and paleohydrogeology preserved in Mexican underwater cave sediments. Quaternary Science Reviews 29, 2788–2798.

Vesica, P.L., Tuccimei, P., Turi, B., Fornós, J.J., Ginés, A., Ginés, J., 2000. Late Pleistocene paleoclimates and sea-level change in the Mediterranean as inferred from stable isotope and U-series studies of overgrowths on speleothems, Mallorca, Spain. Quaternary Science Reviews 19, 865–879.

Vollbrecht, R., 1996. Postglazialer Anstieg des Meeresspiegels, paläoklima und hydrographie, aufgezeichnet in sedimenten der Bermuda inshore waters. Universität Göttingen. 383 pp.

Voβ, M., Struck, U., 1997. Stable nitrogen and carbon isotopes as indicator of eutrophication of the Oder river (Baltic Sea). Marine Chemistry 59, 35–49.

Wang, Y., Cheng, H., Edwards, R.L., Kong, X., Shao, X., Chen, S., Wu, J., Jiang, X., Wang, X., An, Z., 2008. Millennial- and orbital-scale changes in the East Asian monsoon over the past 224,000 years. Nature 451, 1090–1093.

White, W.B., 2007. Cave sediments and paleoclimate. Journal of Cave and Karst Studies 69 (1), 76–93.

Woodward, J.C., Goldberg, P., 2001. The sedimentary records in Mediterranean rockshelters and caves: archives of environmental change. Geoarchaeology 14 (4), 327–354.

Wurster, C.M., Patterson, W.P., McFarlane, D.A., Wassenaar, L.I., Hobson, K.A., Beavan-Athfield, N., Bird, M.I., 2008. Stable carbon and hydrogen isotopes from bat guano in the Grand Canyon, USA, reveal Younger Dryas and 8.2 ka events. Geology 36, 683–686.

Yamamoto, N., Kitamura, A., Irino, T., Kase, T., Ohashi, S., 2010. Climatic and hydrologic variability in the East China Sea during the last 7000 years based on oxygen isotopic records of the submarine caverniculous micro-bivalve *Carditella iejimensis*. Global and Planetary Change 72 (3), 131–140.

Yuan, D., Cheng, H., Edwards, R.L., Dykoski, C.A., Kelly, M.J., Zhang, M., Qing, J., Lin, Y., Wang, Y., Wu, J., Dorale, J.A., An, Z., Cai, Y., 2005. Timing, duration, and transitions of the last interglacial Asian monsoon. Science 304, 575–578.

Zinke, J., Reijmer, J.J.G., Taviani, M., W., D., Thomassin, B., 2005. Facies and faunal assemblage changes to the Holocene transgression in the Lagoon of Mayotte (Comoro Archipelago, SW Indian Ocean). Facies 50, 391–408.